Developing microfluidics and microscopy approaches to investigate bacterial populations with single-cell resolution

Submitted by

Simona Frustaci

to the University of Exeter as a thesis for the degree of Master by Research in Biological Science

(October 2017)

This thesis is available for Library use on the understanding that it is copyright material and that no quotation from the thesis may be published without proper acknowledgement.

I certify that all material in this thesis which is not my own work has been identified and that no material has previously been submitted and approved for the award of a degree by this or any other University.

Simona Frustaci

Abstract

Failures in antibiotic treatments for bacterial infections are typically attributed to antibiotic resistance. However, it has long been realised that bacteria can also employ other mechanisms to aid survival in the presence of antibiotics. Indeed, some bacterial cells react to the presence of antimicrobial drugs by blocking or retarding growth. These cells are named persister cells and can survive bactericidal antibiotics that require active growth for killing. This property is known as “persistence”.

Increasing evidence suggests a link between specific environmental conditions and the development of persistence.

In this study, the temporal windows during the growth cycle when the fraction of persisters to β-lactams, quinolones or aminoglycoside increases have been investigated. Our results confirmed that the environment plays a significant role in persister cell formation. Indeed, cells treated with antibiotics but without fresh media, regrow at a higher density than the cells in the nutrient-rich environment. Nowadays classic microbiological approaches are not sufficient for the study of persister cells, since the persister frequency is often low and dynamic changes in phenotype cause cells to switch between the persister and normal phenotype. Over the past decade, microfluidic techniques have gained increasing interest in the research community. Integrated micro- and nanofluidic lab-on-a-chip systems able to handle samples in a picoliter range are now available, and are certain to become an everyday item in biotechnology and biomedicine within a few years. Here we present a novel microfluidic-microscopy assay for the study of persister cell formation under controlled delivery of antibiotics. Our device is fabricated from polydimethylsiloxane, PDMS, and is able to trap single cells. The microfluidic setup has been integrated with a microscope in order to obtain high-resolution imaging and quantitatively measure growth and shape changes of large numbers of individual cells. Our device allowed us to challenge a culture of *E. coli* with three different antibiotics, and record the individual response of thousands of bacteria. When fresh media was given we distinguished not only dividing cells, as *per* classic microbiological techniques, but also two further phenotypes: elongating and non-growing.

Furthermore, a preliminary study has been conducted regarding the possibility of combining DNA-PAINT with microfluidics for the future investigation of persister cells, with sub-cellular resolution. Together, the results from this thesis enable future investigations, with the goal of advancing our understanding of persistence in response to antibiotics.

Table of contents

List of Figures

List of Tables

List of abbreviation

(p)ppGpp: guanosine pentaphosphate
AHL: N-3-oxo-C6-homoserine lactone
BSA: bovine Bovine serum Serum albuminAlbumin
CAD: computer aid design
CFU: colony forming unit
ddH_2O: double distilled purified water
DNA-PAINT: DNA points accumulation for imaging in nanoscale topography
EDTA: Ethylenediaminetetraacetic acid
GC/MS: gas chromatograph-mass spectrometer
IDT: Integrated DNA Technologies
LB: Luria-Bertani broth
MDK_{99}: minimum duration of treatment that is necessary to kill 99% of a bacterial population
MIC: minimum inhibitory concentration
MM: mother machine chip
PBPs: penicillin-binding proteins
PBS: Phosphate Buffer Solution
PDMS: poly (dimethylsiloxane)
PG: peptidoglycan
PI: propidium iodide
PPK: polyphosphate kinase
PPX: exopolyphosphatase
SEM: standard error of the mean
TA: Toxin-Antitoxin
TE: Tris-EDTA
VBNC: viable but not culturable
WT: wild-type

1. Introduction

The discovery of antibiotics dates back to 1941 and is considered one of the most significant milestones in modern medicine (Cruickshank et al., 2014). In the last 70 years, the treatment of infectious disease has witnessed an extraordinary reduction in the morbidity and mortality mostly due to the rapid development of safe and effective antibiotic drugs. Seen initially as truly miraculous drugs, access to the first available systemic antibiotics (sulphonamides and penicillin) was not immediately available to the public (Alanis, 2005). In fact, these drugs were scarce, very expensive and were initially reserved for use by the military during World War II (Lerner, 2004). As more antibiotics were discovered, manufacturing processes were simplified, and newer formulations developed. Access to antibiotics then eased considerably, and their use became widespread (Alanis, 2005).

However, in an interview with The New York Times in 1945, Sir Alexander Fleming already warned that the inappropriate use of penicillin could lead to the selection of resistant ‘‘mutant forms’’ of *Staphylococcus aureus*. Indeed, the first resistant organisms appeared in 1940 in the form of a *Balantidium coli* strain able to produce an enzyme to disrupt penicillin activity (Abraham & Chain, 1940). Furthermore, in the early 1950s, due to the widespread use of this antibiotic, a significant number of strains of *S. aureus* became resistant to penicillin (Appelbaum, 2006; Ainsa, 2002). Unfortunately, things have not improved in the recent past; every day more bacteria, previously susceptible to common antimicrobials, are reported to have acquired mutations making them resistant to different antibiotics (Alanis, 2005).

However, it is known that some bacteria can avoid killing by certain antibiotics without the mutation. In 1944 Joseph Bigger observed that *S. aureus* could survive extensive antibiotic treatments without acquiring a single resistance mutation. This phenomenon has been called ‘tolerance’ (Horne & Tomasz, 1977) or ‘persistence’ (Bigger, 1944). These terms were coined to distinguish these modes of survival from 'resistance' and have often been used interchangeably in the literature. However, more recently tolerance and persistence have been classified as two different phenomena (Brauner et al., 2016). To briefly summarise why: tolerance and persistence have several common traits, both terms describe a phenotypic variant of susceptible cells which are able to survive

the exposure to high concentrations of antibiotic drugs. Both tolerant and persistent cells are able to re-initiate growth after the drug treatments end. However, Brauner et al. describe the difference being that tolerance generates across an entire bacterial population, while persistence is, by definition, characteristic of a small subpopulation (usually <0.001%) (Brauner et al., 2016). One further mode in which bacterial cells escape stressful conditions is by adopting a viable but not culturable (VBNC) state. Discovered in the 80s (Xu et al., 1982) the VBNC state has been described as a “non recoverable state of existence”. Indeed, VBNC cells, despite being metabolically active at low levels, do not re-initiate growth, even when exposed to ideal conditions.

More details about tolerance, persistence and the VBNC state are described in the section below.

1.1 Drug resistance, tolerance and persistence

1.1.1 Resistance

The term antibiotic resistance is used to describe the heritable ability of microorganisms to grow at high concentrations of an antibiotic (Scholar & Pratt, 2000), irrespective of the duration of treatment. Resistance can be quantified by the minimum inhibitory concentration (MIC) of a particular antibiotic. The MIC is measured by exposing a bacterial population to increasing concentrations of the antibiotic. This allows the measurement of the minimum concentration at which growth is not detected. The MIC for a bacterial strain resistant to an antibiotic is substantially higher than the MIC for an antibiotic-susceptible strain (Brauner et al., 2016). Resistance mechanisms have been studied for a long time and are generally well understood (Eliopoulos et al., 1986; Payne et al., 2007). Fig 1.1 depicts five representative mechanisms.

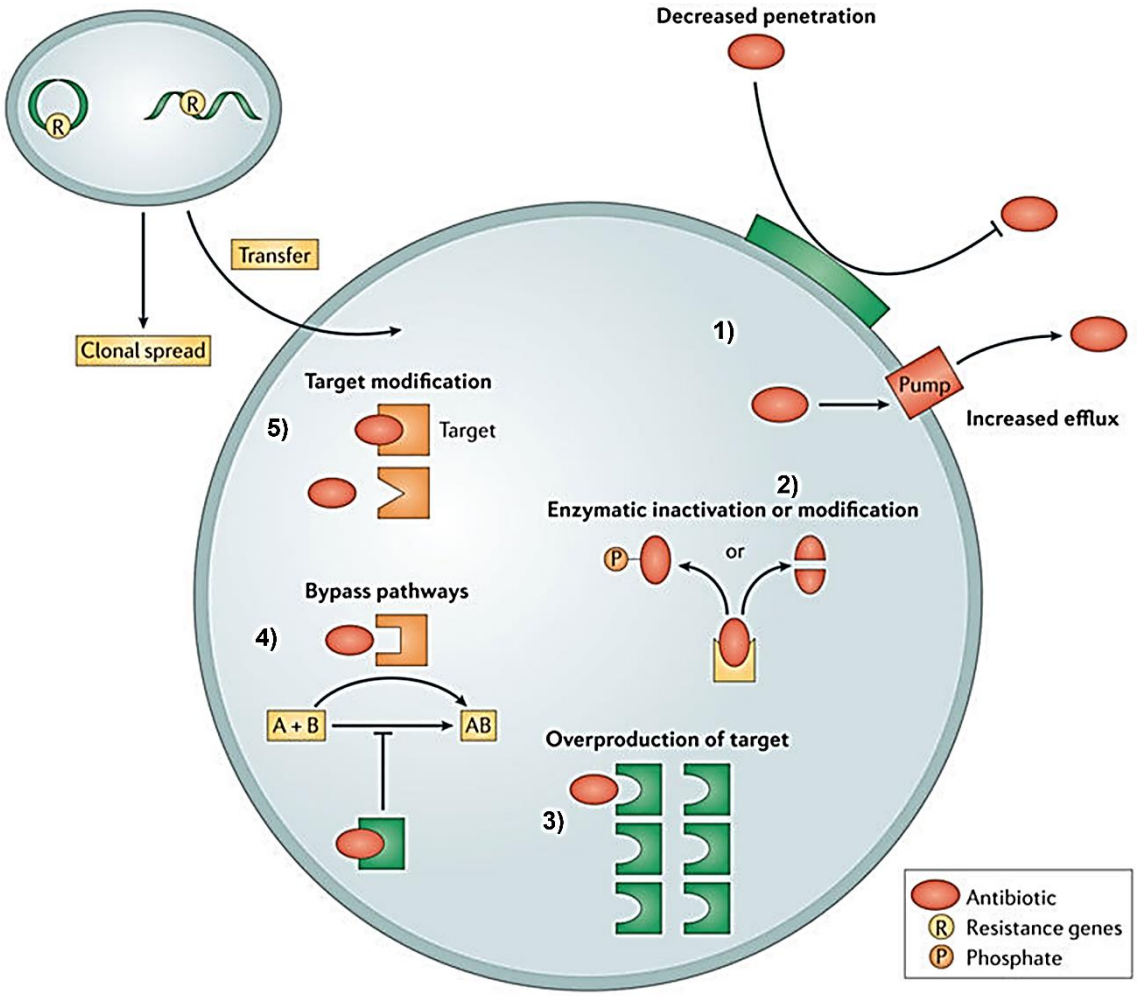

Fig 1.1: A schematic representation of different mechanisms of resistance. 1) restricted penetration and/or efflux of the drug; 2) destruction or inactivation of the antibiotic; 3) overproduction of the antibiotic target; 4) generation of an alternative pathway to avoid the negative antibiotic effect; 5) target modification. Image adapted from Lewis, 2013.

Some bacteria react to antibiotic challenge by the destruction of the antibiotic molecules (for example, by β-lactamases) or target modification (for example, a mutation in the 30S ribosomal protein RpsL confers resistance to streptomycin). An alternative resistance mechanism relies on limited penetration and/or efflux of the drug (Alekshun & Levy, 2007; Walsh, 2003). Furthermore, antibiotic-resistant bacteria are then able to transfer copies of DNA that code for a mechanism of resistance to other bacterial cells, making resistance genes hereditary and transferable, even across distantly related bacteria (Hussain, 2015).This process is called horizontal gene transfer and allows the DNA of resistance genes to spread rapidly across different species.

1.1.2 Tolerance

The term tolerance is used to describe the ability of a microorganism population to survive short exposure to high concentrations of drugs. Tolerance is typically achieved through the slowing down of a bacterial cell's metabolic processes. This can affect the action of all antibiotics which act on growing cells (e.g. β-lactam, fluoroquinolone). Tolerant cells do not carry mutations. However, some studies argue that tolerance can be inherited, as is the case for bacterial species which are inherently slow growing (Brauner et al., 2016). Tolerant bacteria are able to survive at antibiotic concentrations far higher than the MIC and can re-initiate growth when an antibiotic treatment ends (Fridman et al., 2014). Drug tolerance is, therefore, a relevant descriptor of response to bactericidal antibiotics but is not applicable to drugs that solely inhibit bacterial growth, without killing (Kester & Fortune, 2014).

When a population of bacteria develops tolerance, there is no change in the MIC; the only difference is the period required for the drugs to achieve the bactericidal effect. Therefore, a useful parameter to study tolerance is the minimum duration of treatment that is necessary to kill 99% of a bacterial population (MDK_{99}) (Fridman et al., 2014). If antibiotic treatment is interrupted before the MDK_{99}, cell growth will resume, returning to its original level.

1.1.3 Persistence

As mentioned before, the key difference between drug tolerance and persistence is that drug tolerance originates in a whole population of bacterial cells while persistence is a characteristic to only a small subpopulation of cells, named persister cells. Persister cells are not mutants; they are phenotypic variants produced stochastically in the population. The relative abundance of persister cells is less than the 0.01% of the total population (Keren et al., 2004).

Like tolerant cells, persister cells have the ability to spontaneously switch back to the normal, nonpersistent state and regain their usual sensitivity to antibiotics. Upon turning back, they are indistinguishable from normal cells (Kussell et al., 2005). Therefore, persister cell progenies are as sensitive to a drug as the parent culture from which the persister was derived (Lewis, 2010; Moyed & Bertrand, 1983; Peng et al., 2016). The mechanisms of persister cell formation have been

at the centre of several recent reviews (Balaban et al., 2013; Maisonneuve & Gerdes, 2014; Harms et al., 2016).

While bacterial persistence is non inherited, the propensity to form persister cells is a genetically evolved trait (Kussell & Leibler, 2005). Indeed, in 1983 Moyed and Bertrand were able to generate a stable *hip* (high persisters) mutant through the intermittent application of high doses of bactericidal antibiotics to a population of chemically mutagenized *Escherichia coli* K12 (Moyed & Bertrand, 1983).

The *E. coli* mutants were found to have mutations in the *hipBA* toxin-antitoxin (TA) module, which encodes HipA, a toxin, and its cognate antitoxin, HipB.

HipA inactivates an essential amino-acyl tRNA synthetase, owing to the accumulation of uncharged tRNAs (Wen et al., 2017).

Generally, TA modules code for two components, a stable toxin that inhibits cell growth and a labile antitoxin that counteracts toxin activity. Under normal growth conditions, antitoxins potently inhibit the activities of their toxins. In contrast, during stress, the antitoxins are degraded, allowing the toxins to interfere and block DNA replication and protein translation. This inhibition results in rapid growth arrest. When HipA is expressed above a threshold set by the abundance of HipB, a stringent response is induced which leads to the induction of a transient growth arrest. Gerdes and colleagues proposed a molecular mechanism for stochastic persister cell formation through the action of TA modules (Fig. 1.2). This shows that the level of guanosine pentaphosphate (p)ppGpp) varies stochastically in a population of exponentially growing cells and that the high (p)ppGpp level in rare cells induces slow growth and persistence. (p)ppGpp triggers slow growth by activating toxin-antitoxin modules through a regulatory cascade, depending on inorganic polyphosphate and Lon protease that degrades antitoxins. This causes the liberation of their cognate toxins, which inhibit translation and thereby induce persistence (Maisonneuve et al., 2013).

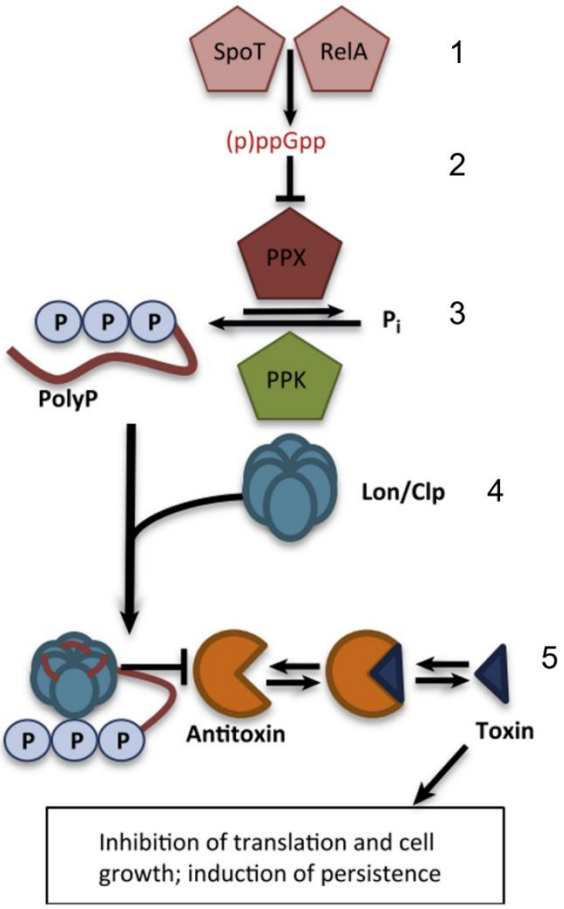

Fig.1.2: Persister cell formation mechanism. 1) Activation of RelA or SpoT causes an increase in intracellular (p)ppGpp levels, 2) resulting in the inhibition of exopolyphosphatase (PPX), the enzyme that degrades PolyP. 3) This results in accumulation of PolyP as a result of the constitutive activity of polyphosphate kinase (PPK). 4) Lon protease is activated by PolyP and begins to degrade antitoxins. 5) Free toxins inhibit translation and cause cells to enter growth arrest and persistence. Image adapted from Ayrapetyan et al., 2015.

The presence of persister cells can be easily detected by the “biphasic killing” of bacterial cultures exposed to bactericidal antibiotics (Fig 1.3).

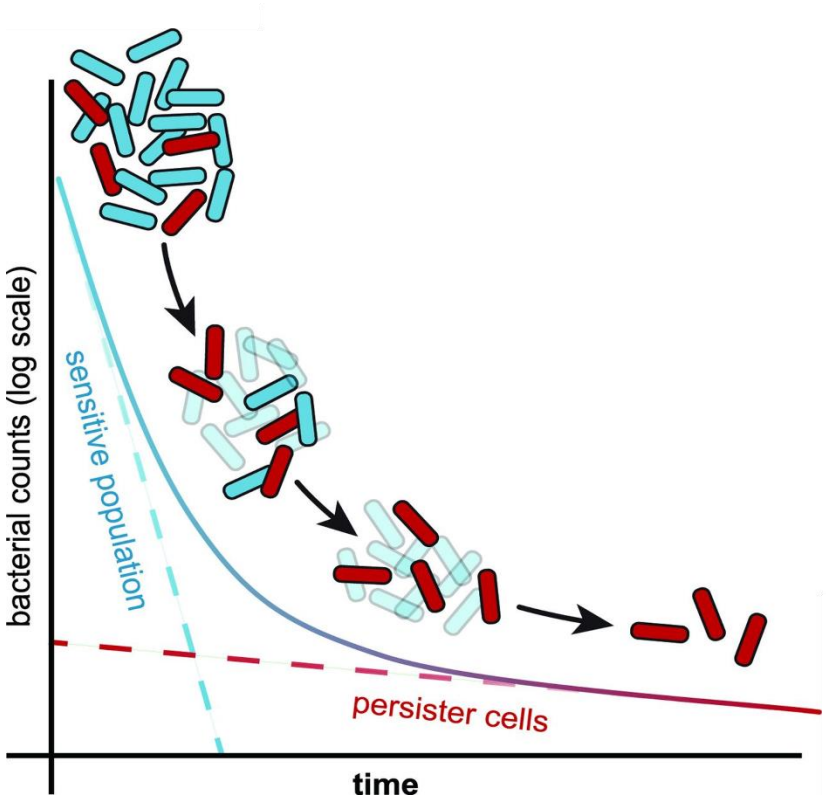

Fig.1.3: A lethal dose of bactericidal antibiotic added at time zero rapidly eradicates the sensitive bulk of the population (blue) until only non-growing persister cells (red) that are killed at a slower rate remain. The termination of antibiotic treatment enables the population to be replenished by regrowth of surviving persister cells. Image adapted from Harms et al., 2016.

After an initial, rapid drop in bacterial counts caused by the effect of the antibiotic on the majority of the cells, the cells are able to initiate a new growth phase when antibiotic concentrations fall (Levin & Rozen, 2006; Harms et al., 2016). In 2004, Balaban and co-workers investigated the formation of persister cells using a microfluidic device, following the response of single cells to drug treatments, whilst entrapped in narrow channels (Balaban et al., 2004). Their study identified two types of persister cells: Type I and Type II. Type I persister cells were generated during the stationary growth phase in response to one or more external triggers. Possible trigger events include starvation, oxidative stress, DNA damage, stressful pH, antibiotics, and interactions with a pathogen (Maisonneuve & Gerdes, 2014).

In contrast, Type II persister cells were produced continuously during growth. Here, a small portion of the cell population remains in a dormant phase, where almost all cell functions are suppressed. This strategy, defined as bet-hedging (Dubnau & Losick, 2006), gives the bacterial population an evolutionary advantage for survival in a changing environment (Maisonneuve & Gerdes,

2014). Both types of persistence represent a threat to human health, and despite being known for a long time, effective strategies for contrasting these cells are still missing.

1.1.4 Viable but non-culturable state

In 1982 Rita Colwell's team described *E. coli* and *Vibrio cholera* cells for the first time to be in a "non-recoverable stage of existence", that remained viable hence metabolically active despite not growing nor dividing (Xu et al., 1982).
Since their discovery at least 85 species of bacteria have been found to enter a mode of dormancy referred to as the viable but non-culturable (VBNC) state (Pinto et al., 2015). Viable but non-culturable (VBNC) bacteria are non-dividing cells that possess low metabolic activity in response to environmental stresses (Kedzierska & Hayes, 2016), including starvation, extreme temperature, low oxygen level and antibiotic exposure (Pinto et al., 2015).
VBNC cells are reported to be viable due to their intact cell membranes, low-level metabolic activity, and continued gene expression. However, they are nondividing and, unlike persister cells, unable to immediately regain the ability to divide when plated on routine laboratory medium. It is worth noticing that both cell types can regrow or resuscitate, ultimately giving rise to a growing population (Ramamurthy et al., 2014).
Despite being closely related, VBNC and persister cells present some differences. VBNC cells are formed after longer periods of incubation in environmental conditions that do not sustain growth (Ramamurthy et al., 2014), while persister cells are formed during growth, albeit at a low frequency (Pinto et al., 2015). However, a recent study (Ayrapetyan et al., 2015) revealed that VBNC cells can exist together with persister cells in unstressed growing cultures, leading to the hypothesis that they form stochastically, with a mechanism similar to Type II persister cells.
Furthermore, changes in the morphology of VBNC cells are extensively documented, as reviewed by Pinto et al., 2015, but no such morphological changes have been reported for persister cells.

1.2 Classes of antibiotics

An antibiotic is an agent that either kills or inhibits the growth of a microorganism. Antibacterial antibiotics are commonly classified based on their chemical structure, mechanism of action, or spectrum of activity. Most antibiotics target bacterial functions or growth processes. Bactericidal antibiotics can target the bacterial cell wall (penicillins and cephalosporins), the cell membrane (polymyxins) or essential bacterial enzymes (quinolones, and sulfonamides). Antibiotics that target the protein synthesis mechanism (macrolides, lincosamides, and tetracyclines) are usually bacteriostatic (except bactericidal aminoglycosides). Figure 1.4 shows the different targets of the major antimicrobial chemoterapic agents.

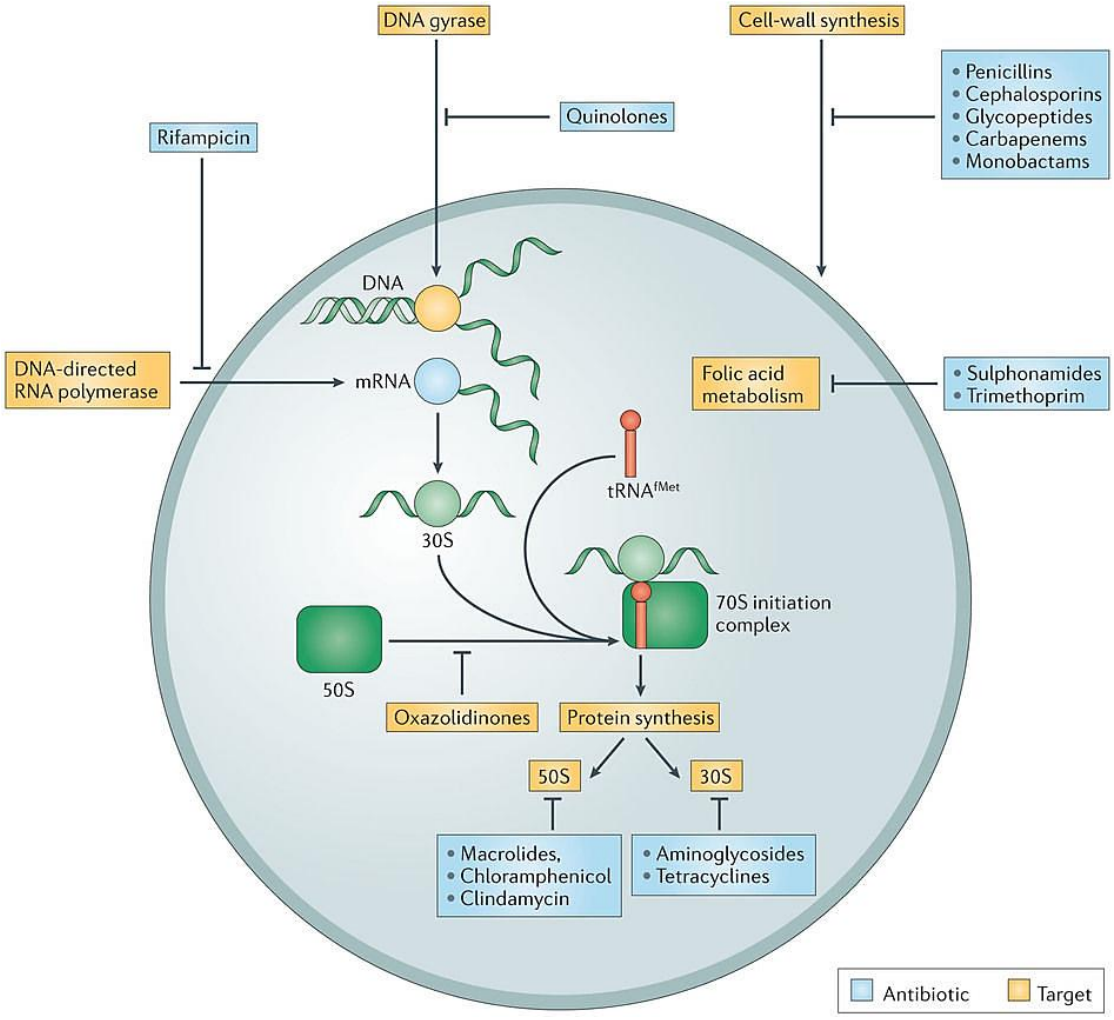

Fig.1.4: Mode of action of the major antimicrobial chemoterapic agents. There are five main antibacterial drug targets in bacteria: cell-wall synthesis, DNA gyrase, metabolic enzymes, DNA-directed RNA polymerase and protein synthesis. The figure shows the antimicrobial agents that are directed against each of these targets. Figure adapted from (Lewis, 2013).

The first antibiotics developed were penicillin and streptomycin, these are both still in use today. Penicillin is now in a class of antibiotics known as the penicillins, which also includes the more recently developed antibiotics ampicillin, flucloxacillin, and methicillin. These antibiotics inhibit the synthesis of the bacterial cell walls, leading to cell lysis and death. Streptomycin is now in the aminoglycoside class of antibiotics, which also contains gentamicin, kanamycin, and netromycin. These antibiotics bind to the 30s subunit of the bacterial ribosome, preventing the synthesis of new proteins. Aminoglycosides are effective against gram-negative bacteria such as *Pseudomonas aeruginosa* and *E. coli*, but they are not active against anaerobic bacteria. Another class of antibiotics that similarly inhibit peptidoglycan synthesis to penicillins is glycopeptides. These antibiotics bind to the amino acids within a cell wall, preventing the addition of new units to peptidoglycan.

Cephalosporins are a broad class of antibiotics. The earliest cephalosporin was isolated by an Italian scientist in 1948 (Partridge, 2009), from bacteria growing in Sardinia. This class of antibiotics has the same mode of action as other β-lactam antibiotics (such as penicillins), but are less susceptible to β-lactamases. Cephalosporins prevent the proper production of a bacterial cell wall by disrupting the synthesis of the peptidoglycan layer forming the cell wall. Early cephalosporins were only active against a few gram-negative bacteria, however, second to fifth generation cephalosporin antibiotics have been designed by biochemists to be effective against a wider range of bacteria. The most recently developed can be used to treat infections caused by gram-positive as well as gram-negative bacteria.

In contrast to the antibiotics mentioned above, tetracyclines and macrolide antibiotics act on the bacterial ribosome. Tetracyclines are protein synthesis inhibitors, blocking the binding of aminoacyl-tRNA to the mRNA-ribosome complex, mainly by binding to the 30S ribosomal subunit in the mRNA translation complex (Chukwudi, 2016).

Erythromycin is probably the most well-known of the macrolide antibiotics, a class which also includes clarithromycin and telithromycin. These inhibit bacterial protein biosynthesis by binding reversibly to the subunit 50S of the bacterial ribosome, thereby inhibiting translocation of peptidyl tRNA.

Quinolones and fluoroquinolones are chemotherapeutic bactericidal drugs, which interfere with DNA replication. Both act by inhibiting the bacterial DNA gyrase or the topoisomerase II enzyme, thereby inhibiting DNA replication and transcription (further detail on this is available in section 1.3.3).

In this study antibiotics from three different classes have been used: a β-lactam, an aminoglycoside, and a fluoroquinolone.

1.3 Antibiotics used in this study

1.3.1 Ampicillin

Ampicillin is a β-lactam antibiotic used to prevent and treat a number of bacterial infections, such as respiratory tract infections, urinary tract infections, meningitis, salmonellosis, and endocarditis. Ampicillin was developed in 1961 (Fischer & Robin Ganellin, 2006) and it is on the World Health Organization's (WHO) List of Essential Medicines, deemed to be the most important medications needed in a basic health system (World Health Organization, 2013). Ampicillin falls within the penicillin group of β-lactam antibiotics and is part of the aminopenicillin family. It is able to penetrate Gram-positive and some Gram-negative bacterial cells. Ampicillin acts as an irreversible inhibitor of transpeptidase, a bacterial cell wall biosynthetic enzyme (Finberg et al., 2012). It inhibits the third and final stage of cell wall synthesis, binary fission, which ultimately leads to cell lysis (Fig 1.5); thus ampicillin is usually bacteriolytic (*American Hospital Formulary Service Drug Information*, 2006; Finberg et al., 2012).

As for other β-lactams, the cellular target of ampicillin is peptidoglycan (PG). This thin layer of biopolymer mesh, which serves to maintain cell morphology and balance turgor pressure. It is composed of long glycan chains and peptide cross-links (Holtje, 1998). Peptide cross-links are formed by the transpeptidase activity of penicillin-binding proteins (PBPs). Ampicillin covalently binds to PBPs and inhibits the formation of cross-links, the final stage of PG synthesis (Tipper & Strominger, 1965).

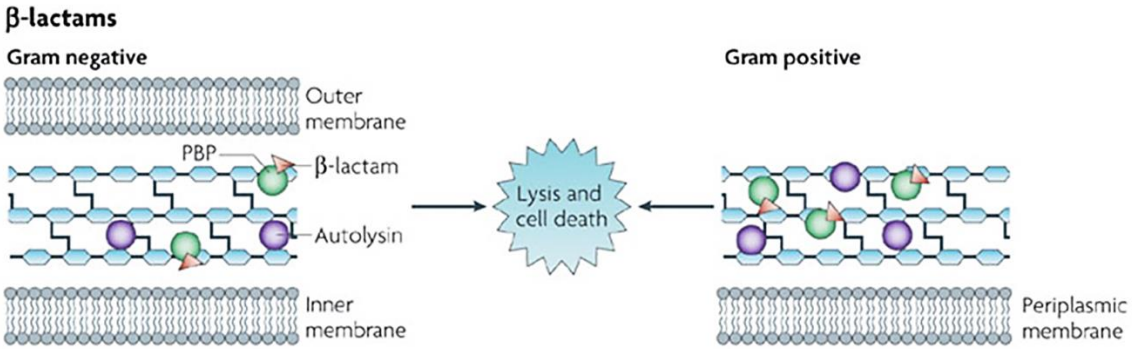

Fig. 1.5: Ampicillin inhibits transpeptidation by binding to penicillin-binding proteins (PBPs) on maturing peptidoglycan strands. The decrease in peptidoglycan synthesis and increase in autolysins leads to lysis and cell death (image adapted from Kohanski, Dwyer, and Collins 2010).

Inhibition of PG synthesis by β-lactams has various effects on cell shape, as PBPs are involved in cell division, elongation, and shape maintenance (Spratt, 1975). It has been proposed that inhibition of cross-link formation by β-lactams combined with misregulated cell wall degradation by PG hydrolases results in an accumulation of PG defects, which ultimately leads to cell lysis (Chung et al., 2009).

1.3.2 Gentamicin

Gentamicin belongs to the aminoglycoside antibiotic family, which is known to be clinically effective in the treatment of most gram-negative aerobic and facultative anaerobic bacilli infections, exerting both a bacteriostatic and bactericidal effect (Hathorn et al., 2014). However, it does not show activity against gram-negative anaerobes and most gram-positive bacteria (Levison, 2012). Aminoglycosides are most effective against bacteria populations that are rapidly multiplying (Boothe, 2012). These activities are attributed to a primary mode of action such as protein synthesis inhibitors. The inhibition of protein synthesis by aminoglycosides is mediated through energy-dependent binding to the cytosolic, membrane-associated bacterial ribosome (Mingeot-Leclercq et al., 1999). Aminoglycosides first cross bacterial cell walls (lipopolysaccharide in gram-negative bacteria) and cell membranes, where they are actively transported (Boothe, 2012). Aminoglycoside presence in the cytosol generally inhibits peptide elongation at the 30s ribosomal subunit, giving rise to inaccurate mRNA translation and therefore biosynthesis of proteins that are truncated (Fig.1.6), or

bear altered amino acid compositions at particular points (Mingeot-Leclercq et al., 1999).

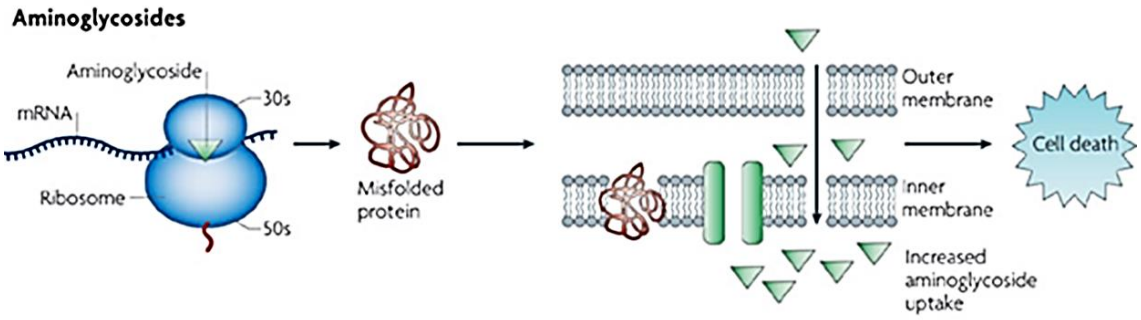

Fig. 1.6: Aminoglycosides bind to the 30S subunit of a ribosome and cause misincorporation of amino acids into elongating peptides. These mistranslated proteins can misfold; incorporation of misfolded membrane proteins into the cell envelope leads to increased drug uptake. This, together with an increase in ribosome binding, has been associated with cell death (image adapted from Kohanski, Dwyer, and Collins 2010).

Specifically, binding impairs translational proofreading, leading to a misreading of the RNA message, premature termination, or both, and so to the inaccuracy of the translated protein product. Proteins misfolded as a result of this are then incorporated into the bacterial cell membrane, which may lead to changes in its permeability, thus enabling further aminoglycoside uptake (Mingeot-Leclercq et al., 1999). The drug's action ends with cell death, caused by the loss of structural integrity in the cell membrane (Boothe, 2012).

1.3.3 Ofloxacin

Ofloxacin is a synthetic antibiotic of the second-generation fluoroquinolone drug class (Kawahara, 1998; Nelson et al., 2007). The fluoroquinolones represent an expanding class of broad-spectrum antibacterial drugs, which target a wide range of Gram-negative and anaerobic species. These bacteria are responsible for many infections, in particular in the ocular region (Hooper, 1999; Smith et al., 2001; Zechiedrich & Cozzarelli, 1995). Fluoroquinolones act by inhibiting two enzymes involved in bacterial DNA synthesis, both of which are DNA topoisomerases. These enzymes are not present in human cells and are essential for bacterial DNA replication, thereby enabling these agents to be both specific and bactericidal. Specifically, fluoroquinolones inhibit DNA gyrase and topoisomerase IV. DNA gyrase introduces negative super-helical twists in the

bacterial DNA double helix ahead of the replication fork, thereby catalysing the separation of daughter chromosomes (Fig. 1.7).

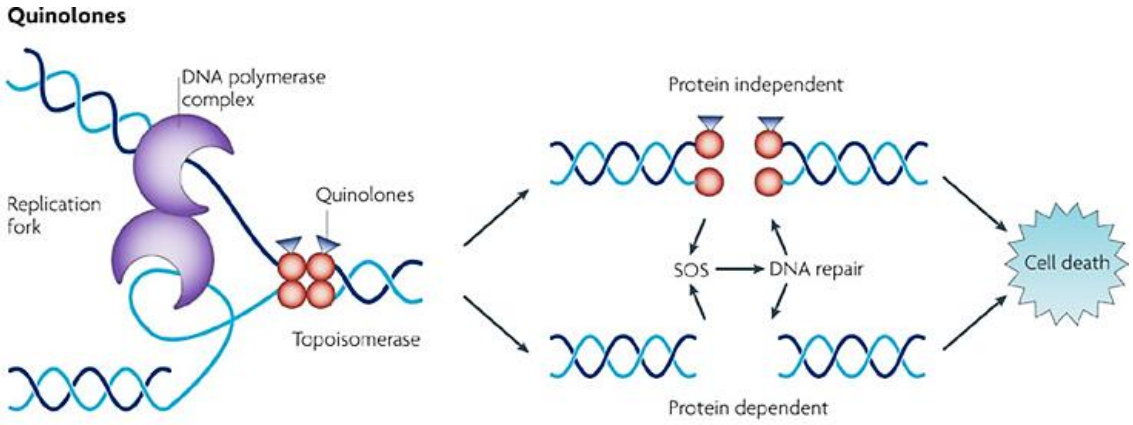

Fig. 1.7: Drug-target interactions and associated cell death mechanisms. Quinolone antibiotics interfere with changes in DNA supercoiling by binding to topoisomerase II or topoisomerase IV. This leads to the formation of double-stranded DNA breaks and cell death in either a protein synthesis-dependent or protein synthesis-independent manner (image adapted from Kohanski, Dwyer, and Collins 2010).

This mechanism is essential for the initiation of DNA replication and allows for binding of initiation proteins (Blondeau, 1999; Pan & Fisher, 1997). Topoisomerase IV is responsible for decatenation, removing the links between chromosomes, thereby allowing segregation into two daughter cells at the end of a round of replication (Zechiedrich & Cozzarelli, 1995). Fluoroquinolones interact with the enzyme-bound DNA complex (i.e., DNA gyrase with bacterial DNA or topoisomerase IV with bacterial DNA) to create conformational changes that result in the inhibition of normal enzyme activity. As a result, the drug-enzyme-DNA complex blocks progression of the replication fork, thereby inhibiting normal bacterial DNA synthesis and ultimately resulting in rapid bacterial cell death (Kampranis & Maxwell, 1998; Marians & Hiasa, 1997).

1.4 Application of microfluidics in microbiology

Microfluidics allows the control and manipulation of fluids contained in small (generally 10–100 μm) channels, where fluid flow is dominated by surface tension and laminar effects (Saleh-Lakha & Trevors, 2010). Microfluidic technologies provide a platform for combining the simplicity of fluidic diffusion with the quantitative measurement of dilutions.

The origin of microfluidic devices is associated with the late 1960s. The first microfluidic device was a prototype of a quadrupole gas chromatograph-mass spectrometer (GC/MS) by Finnigan Instrument Corporation, who sold it to Stanford and Purdue University. This first instrument cost 100,000 USD, and was controlled by a mini-computer (Brock, 2011).

In 1993, Andreas Manz published a pioneering article describing the fabrication of a miniaturised capillary electrophoresis-based chemical analysis system on a chip (Harrison et al., 1993). Only one year after the publication of Manz's work, the first International Conference on Micro-Total Analysis Systems took place in Enschede, the Netherlands, as a forum for reporting the latest research in the field of microfluidics, including: Lab-on-a-Chip, microfabrication, nanotechnology, integration and detection technologies for life sciences and chemistry.

Professor George Whitesides, one of the major and more active pioneers of microfluidics as a technique, published an article in 1998 on the rapid prototyping of microfluidic systems in polydimethylsiloxane (PDMS). This publication described the design and fabrication of microfluidic chips for capillary electrophoresis in a transparent, elastomeric material. Such chips could be made in less than a day using high-resolution printing, contact lithography, moulding of PDMS, and contact sealing of oxidised PDMS surfaces. (Duffy et al., 1998; Xia & Whitesides, 1998). Whiteside's work had a large impact on the microfluidics community. It allowed a user to design the microfluidic channels directly, using a CAD program. Furthermore, microfluidic devices fabricated from PDMS are physically robust and inexpensive, with fast and straightforward sealing of channels in oxidised PDMS.

Subsequently, the group of Dr Richard D. Fair at Duke University (USA), published an article on the rapid actuation of discrete liquid droplets accomplished by direct electrical control of the surface tension (Pollack et al., 2000). It was the first publication describing a liquid handling technology known

as digital microfluidics. This novel method had a massive influence on chemical and enzymatic reactions, DNA-based applications, immunoassays, clinical diagnostics, cell-based applications and proteomics, due to flexible device geometry, simple instrumentation, and easy integration with other technologies (Choi et al., 2012).

Microfluidic devices applied in the field of microbiology offer significant improvement over traditional methods. Microfluidic devices are now easy to fabricate, require little power and require lower reagent consumption. They have the capability to handle high-throughput analyses and allow precise handling of small liquid volumes in microchannels (10–1000 μm).

In recent years, microfluidic systems have offered an attractive method for automating the process of DNA and RNA extraction (Vulto et al., 2010) and for the preparation of DNA libraries (Yehezkel et al., 2016). Analysis of the phenotype and behaviour of a bacterial system can also be automated and carried out at the single-cell level (Guo et al., 2012). This has made microfluidics particularly useful for studying bacterial interactions, as a small number of cells can be grown under precise conditions, with tightly controlled and predictable fluid flow rates. In 2016, Ramalho and co-workers described a microfluidics-based approach for the single-cell analysis of bacterial sender and receiver systems, based on *E. coli*, engineered with the quorum sensing systems of *Aliivibrio fischeri* (Ramalho et al., 2016). This approach allowed the dynamic response of receiver bacteria to varying amounts of the quorum sensing inducer N-3-oxo-C6-homoserine lactone (AHL) to be studied in terms of gene expression. Developing the testing of susceptibility to antibiotics in a microfluidic scale carries the advantage of practical sample usage, since it requires small sample quantities. At the same time, microfluidic devices are easily scalable to perform multiple tests on multiple samples (Mairhofer et al. 2009; Sauer-Budge et al. 2009; Yager et al. 2006).

The research of Balaban's group led to a mathematical model which describes the persister phenotypic switch. They found the optimal rate of switching between a normal or persister cell phenotype to depend strongly on the frequency of environmental changes, and only weakly on the selective pressures of any given environment (Balaban et al., 2004; Kussell et al., 2005). More recent studies used a microfluidic device to show that Wild Type (WT) *E. coli* becomes persistent by temporarily switching into a slow growth state. The switch happens in rare cases

where a cell has a high enough level of (p)ppGpp to activate the regulatory cascade responsible for growth arrest (Maisonneuve et al., 2013). They also reveal the regulatory network behind this mechanism of switching.

Campos et al. (2014) and Taheri-Araghi et al. (2015) used a combination of microfluidics and microscopy to better study single cell growth and size during a replication cycle. This study requires precise measurement of the size (length) of many cells grown under steady-state growth conditions. The two groups were able to maintain constant growth conditions over an extended period of time, so that cells could be imaged and analysed over several generations. Many cells were tracked simultaneously. Measurements of cell length from birth to division were obtained with high precision at the single-cell level.

The microfluidic chip used by Taheri-Araghi, et al. (2015) is known as the Mother Machine. The Mother Machine (section 2.2.2) was developed by Jun and colleagues, and its design is publicly accessible on the Jun lab's website (Taheri-Araghi et al., 2015; Wang et al., 2010; http:// jun.ucsd.edu/, Method 1 in Section 11). The Mother Machine has individual growth channels similar to those used by Balaban et al. (2004). Each chip can contain over 1000 growth channels. One end of each channel is closed, and the other end opens into the main channel, where growth medium flows through. A cell at the closed end of the growth channel is referred to as the 'mother cell'. The size of the growth channels is designed to match the average diameter of the bacteria, to prevent the mother cell from moving around, making image analysis and cell tracking much easier.

All these studies have significantly enriched microfluidics-based research. In particular those focused on bacterial phenotyping, and responses to external environmental stimuli.

1.5 DNA-PAINT

Much of our knowledge regarding biological processes at the cellular and subcellular level has come from direct cell imaging. Fluorescence microscopy is one of the most widely used imaging techniques because of its two principal advantages: specific cellular components may be observed through molecule-specific labelling, and when combined with light microscopy, allows the observation of structures inside a live sample in real time (Huang et al., 2008). However, conventional fluorescence microscopy is limited by relatively low spatial resolution, due to the diffraction limit of light. This limit is about 200–300 nm in the lateral direction and 500–700 nm in the axial direction (Huang et al., 2009). In recent years, a number of “super-resolution” fluorescence microscopy techniques have been invented to overcome the diffraction barrier. High-precision localisation of bright light sources, such as fluorescent particles, is often used in biophysical experiments (Mohan et al., 2013).

1.5.1 Super resolution fluorescence microscopy

A biological structure is defined by the positions of the atoms that build up the structure of the molecules. In the same way, a fluorescence image is defined by the spatial coordinates of the fluorophores that generate the image. The position of an isolated fluorophore can be precisely determined through the detection of the photons emitted; the more photons recorded, the more precise the localisation (Huang et al., 2008). Taking advantage of single-molecule detection and imaging (Moerner & Kador, 1989; Orrit & Bernard, 1990), nanometre-precision in the localisation of single fluorescent molecules has also been achieved (Yildiz, 2003).

When multiple molecules are present in close proximity, however, localisation becomes inaccurate or impossible because the images of these fluorophores overlap. Separation of the fluorescence signal from a few molecules with overlapping images may be achieved either in the spectral domain, according to their distinct excitation or emission spectra (Churchman et al., 2005; Lacoste et al., 2000; van Oijen et al., 1998) or in the time domain, taking advantage of the photo-bleaching (Gordon et al., 2004; Qu et al., 2004), or blinking (Lagerholm et al., 2006; Lidke et al., 2005) of the different emitters. It is, however, difficult to

scale up the number of fluorophores that can be resolved within a diffraction-limited area using these methods.

Molecules can ‘switch’ between fluorescence on- and off-states to obtain sub-diffraction image resolution (Jungmann et al., 2014). This switching is traditionally obtained in two ways: the first, providing targeted switching, actively confines the fluorescence excitation to an area smaller than the diffraction limit of light, while in the second, switching is stochastic, making use of photo-switchable proteins or organic dyes.

1.5.2 DNA-PAINT and microfluidics

The technique termed universally PAINT (Point Accumulation for Imaging in Nanoscale Topography) achieves specific dye-sample interactions, but lacks the ability to specify interactions with programmable kinetics. In a similar manner to PAINT, DNA intercalating dyes have also been used to obtain super-resolved images of DNA (Flors et al., 2009; Schoen et al., 2011). Here, imaging is carried out using diffusing fluorescent molecules that interact transiently with the sample (Jungmann et al., 2014). Illustrated for the first time by Jungmann et al.,(2014), DNA point accumulation for imaging in nanoscale topography (DNA-PAINT) is a new technique developed to overcome the diffraction limit for super-resolution imaging. DNA-PAINT is represented by stochastic switching (Fig 1.8). Imaging is carried out using diffusing fluorescent molecules bonded with single stranded DNA (ssDNA), known as imager strands, which interact transiently with complementary ssDNA (docking strands). Docking strands are short, single-stranded DNA oligomers, usually 8–10 nucleotides long. These can be fixed to a biological target of interest, using standard immune-labelling approaches with DNA-conjugated antibodies, as illustrated in Fig.1.9, targeting proteins of interest (Agasti et al., 2017) or direct hybridisation of docking strands to DNA or RNA molecules. In contrast, the imager strand is conjugated to an organic dye and diffuses freely in the imaging buffer. Usually, imager strands are hard to detect because they diffuse over many camera pixels during the duration of a single time frame. However, thanks to their complementary sequence, imager strands can transiently bind to docking strands. During the bound state, imager strands are fixed for an extended amount of time, allowing the camera to accumulate enough photons from the dye to be detected (Schnitzbauer et al., 2017).

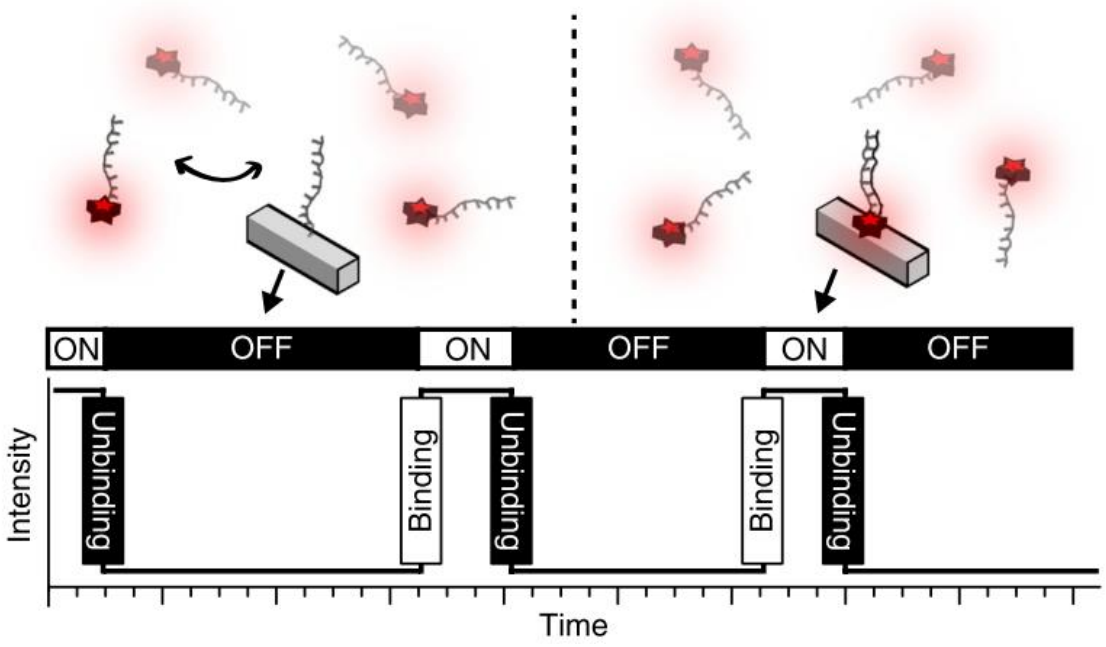

Fig 1.8: DNA-PAINT concept. Transient binding of dye-labelled DNA strands (imagers) to their complementary target sequence (docking site) attached to a molecule of interest. The transient binding of imager strands is detected as 'blinking', illustrated by the intensity versus time trace (Schnitzbauer et al., 2017). Red stars represent dyes.

DNA-PAINT is not prone to photobleaching as imager strands are continuously replenished from the solution; the binding duration depends exclusively on the stability of the formed DNA duplex, and can hence be programmed by modulating strand length, GC content, temperature or salinity of the imaging buffer. The affinity of imager strands for docking strands is nearly 100%, and allows sequential imaging of multiple targets using one dye and one laser, in fact, DNA-PAINT does not require special experimental conditions to obtain photo-switching, so long as probes are able to diffuse freely and reach their targets.

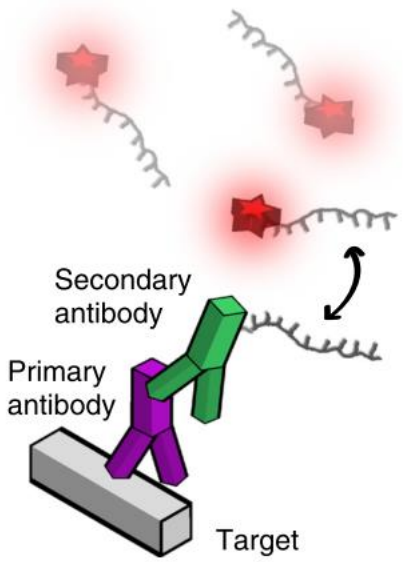

Fig. 1.9: *In situ* protein-labelling strategy for DNA-PAINT using primary and DNA-conjugated secondary antibodies (Schnitzbauer et al., 2017). Red stars represent dyes.

DNA-PAINT brings several advantages. First, the use of DNA-based imaging probes enables high multiplexing, as seen *via* Exchange-PAINT (Jungmann et al., 2014). After the first DNA-PAINT image has been acquired, the imager solution can be washed away with buffer and replaced by a different imager solution. Repeated imaging, washing and reintroduction of new imager strand species allows the creation of a multiplexed image of different biological targets. Furthermore, by programming the binding duration, an extremely high number of photons can be detected from a single binding (or blink) event, enabling optimal localisation precision. The predictability of DNA binding and unbinding events, combined with effectively no bleaching allows accurate quantitative imaging.

As Jungmann demonstrated, buffers play a major role in DNA-PAINT. By employing a microfluidic experimental set-up, buffers can be continuously exchanged, and different types of imager/fluorophores can be replaced and tested in a fast and efficient manner. Thus, the sample is never moved from the stage, and all solutions are added and removed *in situ*, enabling systemic analysis of all the different combinations tested, advancing possibilities for technical development and novel biological applications.

1.6 Project aims

The overall aim of this project is to develop a series of new methods which will allow a better understanding of antibiotic persistence and the VBNC state in the model bacterium *E. coli. E. coli* has long been one of the favoured model organisms in molecular and genetic studies because of the deep knowledge of its genome and genetic regulation mechanisms, and the ease with which it can be handled and studied in a laboratory setting. For this thesis, classic microbiological techniques have been used.

In the first part of this project, cultures of *E. coli* have been treated with three different antibiotics: ampicillin, gentamicin and ofloxacin. These antibiotics were supplemented with a solution either containing fresh nutrient media or the medium spent by the growing bacterial culture itself, in order to study the formation of persister cells. Furthermore, the role of the gene *ompF* in the formation of persister cells has been investigated. In parallel to this, a microfluidic-microscopy approach has been developed to study a cell's response to the stress caused by the exposure to the aforementioned antibiotics at single-cell resolution.

The second part of this project focused on preliminary work with the technique of DNA-PAINT coupled with microfluidics and fluorescence microscopy. The sequences for docking strands and imager strands were designed, and then a microfluidic chip was moulded to perform an EXCHANGE-PAINT experiment.

The rationale behind this project is to develop the techniques of DNA-PAINT, microfluidics, and super-resolution microscopy to study the physiology of normal, persister, and VBNC cells, and the phenotypic responses of these cell states to environmental stimuli, in this case, the presence of antibiotic compounds. Taken together these studies will especially enrich knowledge of persister cell formation providing novel and relevant information about the persister phenotype.

2. Materials and Methods

All chemicals were obtained from Sigma-Aldrich (Irvine, UK) unless otherwise stated. All chemicals used were of analytical grade. All solutions were made using Purite double distilled purified water (ddH_2O). All media and buffers used in microbiology were sterilised by autoclaving at 121 °C for 20 minutes at 15 psi, or by filter sterilisation using a Sartorius Stedim, minisart 0.2 µm single-use filter unit (Sartorius, Stonehouse, UK).

2.1 Microbiology

2.1.1 Growth media

Table 2.1: Media used in this study

***E. coli* Media**	**Components (for 1 L)**	
Luria-Bertani (LB) broth	10 g 10 g 5 g	Tryptone NaCl Yeast extract
LB agar	1 L 8 g	LB Broth Agar
M9 Minimal Medium (M9)	12.8g *OR* 6 g 3 g 0.5 g 1 g	$Na_2HPO_4 \cdot 7H_2O$ Na_2HPO_4 (anhydrous) KH_2PO_4 NaCl NH_4Cl

2.1.1.1 Spent LB

Spent LB was made by two sequential centrifugation steps at 4000 rpm for 5 minutes and a 0.2 µm filtration steps from an overnight culture (17 hours) before re-inoculation with bacterial cells.

2.1.2 Antibiotics

Antibiotics were prepared at a 1000× concentration in ddH_2O. Stocks were stored at -20 °C and fully defrosted before use. Three different antibiotics have been used: Ampicillin, Gentamicin, and Ofloxacin. Final working concentrations used in each assay was 25 × minimal inhibitory concentrations (MIC). Table 2.2 shows MIC literature versus MIC found in our laboratories through different experiments.

Table 2.2: MIC literature versus MIC determined in our laboratories through different experiments.

E. coli K-12 BW25113 wild-type	Minimum inhibitory concentration (MIC)			
	96-well assay Mean ± SEM	**MIC test strips** Mean ± SEM	**Literature**	**25× MIC**
Ampicillin (µg/mL)	5.00 ± 1.00	4.66 ± 1.33	3 (“Eurofins Scientific,” 2017) 5 (X. Guo et al., 2013) 2 (Ma et al., 2009) 16(Firmino et al. 2013)	125
Gentamicin (µg/mL)	4.00 ± 1.09	0.54 ± 0.23	1(“Eurofins Scientific,” 2017) 4 (Ma et al., 2009)	100
Ofloxacin (µg/mL)	0.125 ± 0.001	0.08 ± 0.01	0.1 (Hansen et al. 2008)(“Eurofins Scientific,” 2017)	3.125

2.1.3 *Escherichia coli* growth

For this study, the strains *Escherichia coli* BW25113 (Dharmacon, Lafayette, CO, USA) and its knock-out derivative Δ*ompF* were used. Luria Bertani (LB) broth and LB agar plates were used to culture *E. coli*. Overnight cultures were prepared by inoculating a single colony from a streak plate to 200 mL of LB broth followed by incubation at 37°C in a shaking incubator (250 rpm) for at least 16 hours.

2.1.4 Classic Microbiological assays

2.1.4.1 Growth curve

An overnight culture of *E. coli* was diluted 1:1000 in 100 mL LB and cultured on a shaker (250 rpm) at 37 ˚C for 8 hours. 500 µL of cells were transferred to an Eppendorf tube for each time point required and centrifuged for 5 minutes at 13000 rpm. Then 470 µL of supernatant was removed, the cell pellets were re-suspended in 470 µL Phosphate Buffer Solution (PBS) and serially diluted. For all time points required 10µL of each cells dilution was spotted on an LB agar plate then plates were incubated in a static incubator at 30°C for at least 16 hours for measuring colony forming units (CFU). Three biological replicates were prepared for each time point.

The Fig. 2.1 shows the control curve of an overnight culture of WT *E. coli.*

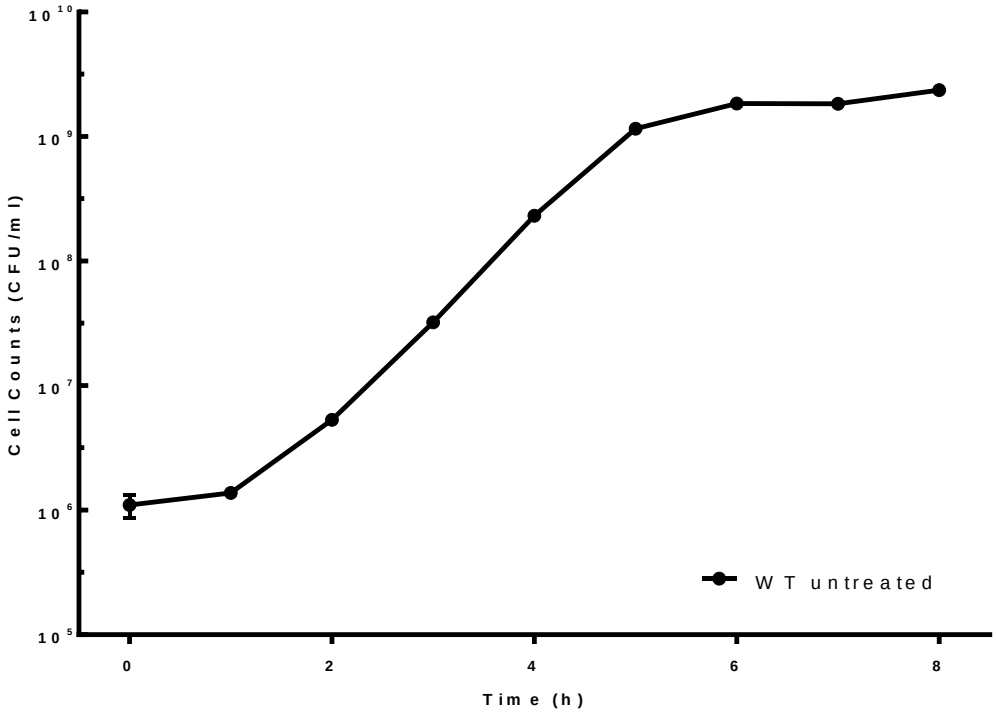

Fig 2.1: An overnight culture of *E. coli* was diluted 1:1000 in LB and cultured on a shaker (250 rpm) at 37 ˚C for 8 hours. Data and error bars are the mean and standard error of the mean (SEM) of measurements obtained by using the colony forming unit (CFU) assay at least on biological triplicates as described in section 2.1.4.1.

2.1.4.2 Persister cells assay

As already mentioned in the Introduction Persister cells are a subpopulation which is able to survive exposure to high concentrations of an antibiotic without devolving a resistance. To allow the selection and study of this fraction of cells an assay has been developed and is illustrated in the figure below.

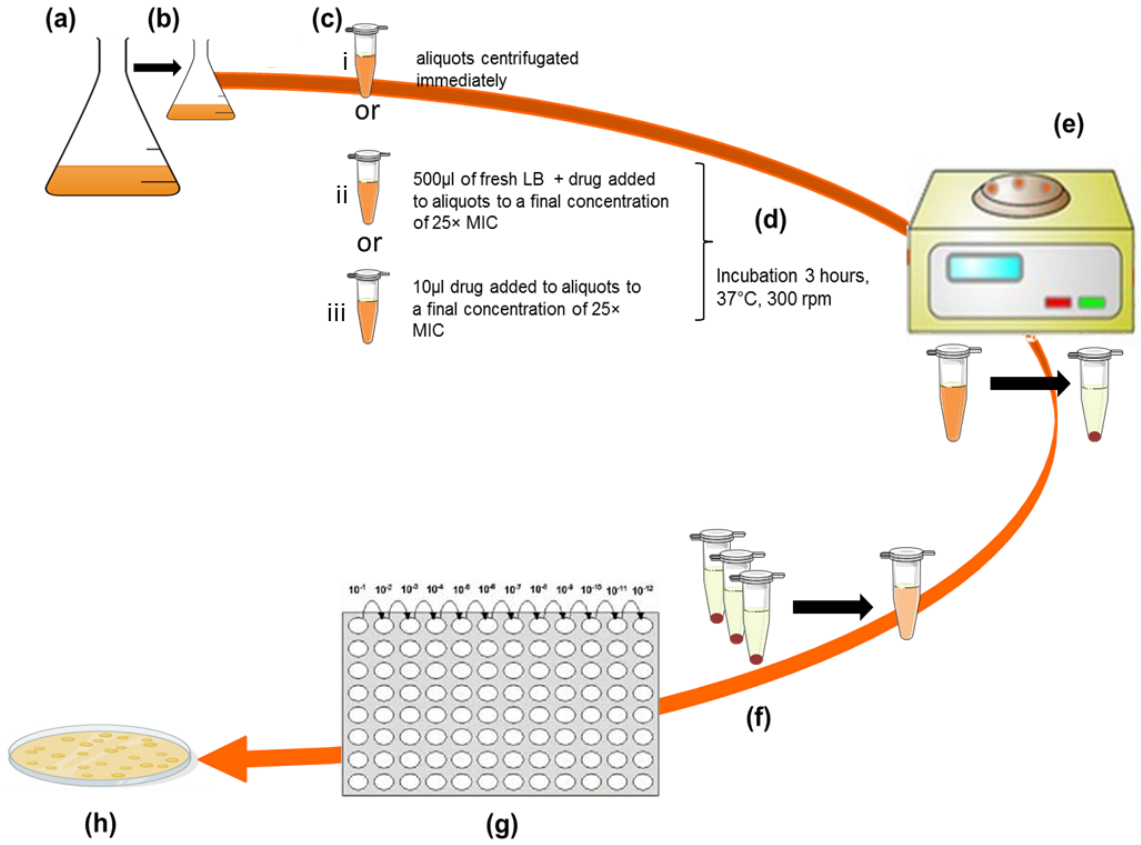

Fig. 2.2: Cartoon illustrating the persister cells assay. A single colony of *E. coli* grew for 17 hours at 37 °C at 200 rpm in LB media (a). t=0 the time at which this culture was diluted 1:1000 in LB and growth at 37 °C and 200 rpm was restarted (b). Nine aliquots were taken from the growing culture every 30 minutes (c). Three aliquots were centrifuged immediately; the other six were treated for 3 hours, three supplemented with 500 µl of fresh LB and three directly to the aliquot. In both cases, the final concentration was 25×MIC. The treated aliquots were incubated for 3 hours at 37 °C and 200 rpm, centrifuged 13000rpm for 5 minutes (e), re-suspended in PBS (f), serial diluted (g) and plated on LB agar (h).

An overnight culture of cells was diluted 1:1000 in 100 mL LB flask and cultured on a shaker (250 rpm) at 37˚C for 8 hours. 500 µL of cells were challenged in Eppendorf tube for each time point required with drug (ampicillin, gentamicin or ofloxacin) in LB or only drug to reach a final concentration of 25× MIC and incubated at 37˚C for three hours. After 3 hours of incubation with the drug, three aliquots were centrifuged for 5 minutes at 13000 rpm, re-suspended in PBS and diluted several times. For all time points required 10 µL of each cell dilution was spotted on an LB agar for determination of CFU then plates were incubated in a static incubator at 30 °C for at least 16 hours. Three biological replicates were prepared for each time point.

2.2 Microfluidics

2.2.1 Soft Lithography

Soft lithography is the general name for several different nanofabrication techniques such as replica moulding, micro-contact printing, micromoulding in capillaries, micro-transfer moulding, solvent assisted micro moulding and near-field conformal photolithography using an elastomeric phase-shifting mask (Madou, 2002). All these methods use an elastomer either as the end product or as an intermediate step as for example as a stamp. The most common elastomer used is PDMS.

In brief, a master initially is produced on a silicon wafer by one of the nanofabrication techniques mentioned above. The masters used in this study were prepared through UV-photolithography. The device layout is printed on a transparency or a chrome mask making some areas transparent and others opaque to UV-light. A silicon wafer is then spin-coated with a photocurable resist which is exposed to UV-light through the mask. The wafer is then subjected to an etching solution that removes the uncured photoresist. The master is ready to be used as a mould to cast a negative structure in an elastomer (Whitesides et al., 2001). The elastomeric replica produced can be used as a component of a microfluidic device or as a stamp to transfer the pattern to a different material. The greatest advantage of soft lithography is that devices can be produced very quickly, at low cost and the end product often has a high quality.

2.2.1.1 PDMS (Polydimethylsiloxane)

PDMS is a polymer which is often used for microfluidic applications. PDMS is flexible, optically transparent to wavelengths >230nm, impermeable to water but not to gases and biocompatible (Sia & Whitesides, 2003). PDMS is made up of repeating units of $–OSi(CH_3)_{2-}$. Its surface is hydrophobic in its unprocessed state due to the CH_3 groups. This is a considerable drawback in microfluidic application since it renders the surface lacking in wettability with aqueous solvents and offers a channel surface prone to trapping air bubbles. The problem of hydrophobic surfaces can, however, be overcome by treating the PDMS structure with an oxygen plasma to render the surface hydrophilic. The mechanism behind the change in susceptibility to water is due to an oxidation of the surface producing silanol groups (Si-OH) at the surface (Bhattacharya et al., 2005). An oxidised PDMS surface will stay hydrophilic if kept in contact with water whereas in the air the hydrophobic groups will once again dominate the surface behaviour in ~30 minutes (Sia & Whitesides, 2003). The capacity to produce hydrophilic silanol surface groups also enables irreversible bonding to silicon-based structures such as glass slides or other PDMS structures.

2.2.2 Device Design

The microfluidic platform was designed in AutoCAD© (Autodesk, San Rafael, CA, USA). Several models were tested were parameters such as width and height of the different channels, the number of and placing of inlets and outlets, as well as connections between inlets and outlets and capillaries were evaluated. Here will be reported chips called Cell chip 2 (Fig. 2.3) and Mother machine chip (Fig. 2.4), which was already available in our laboratory.

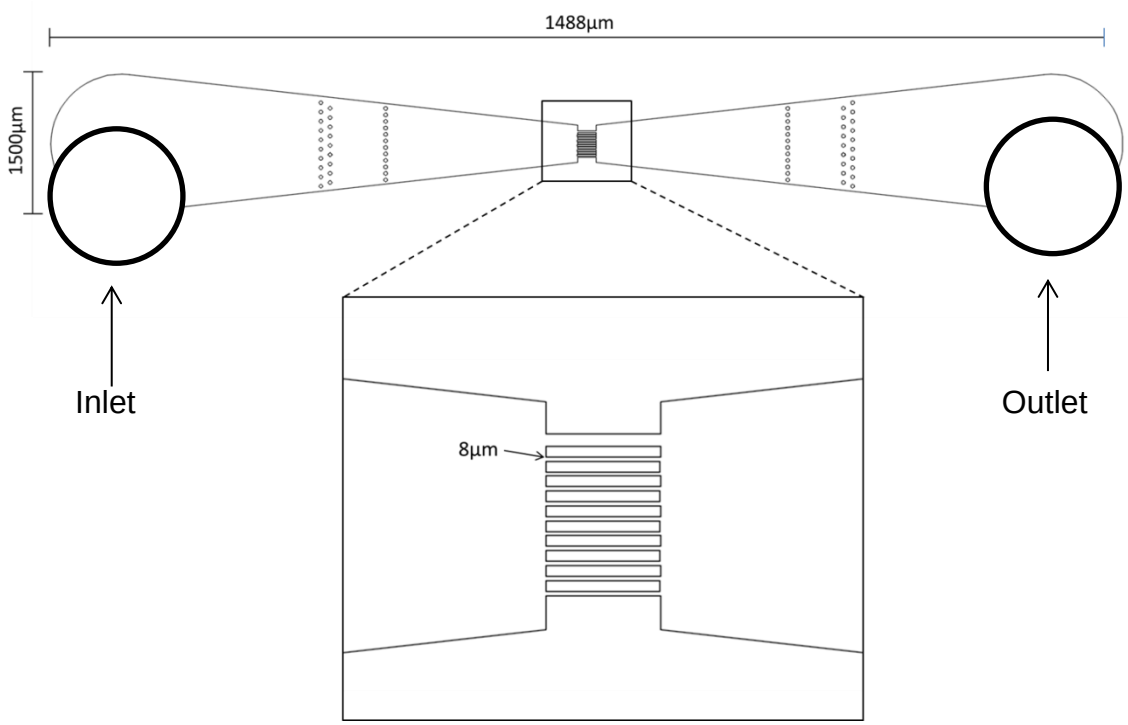

Fig.2.3: The Cell chip 2 design of the photomask (top) and its channels (bottom).

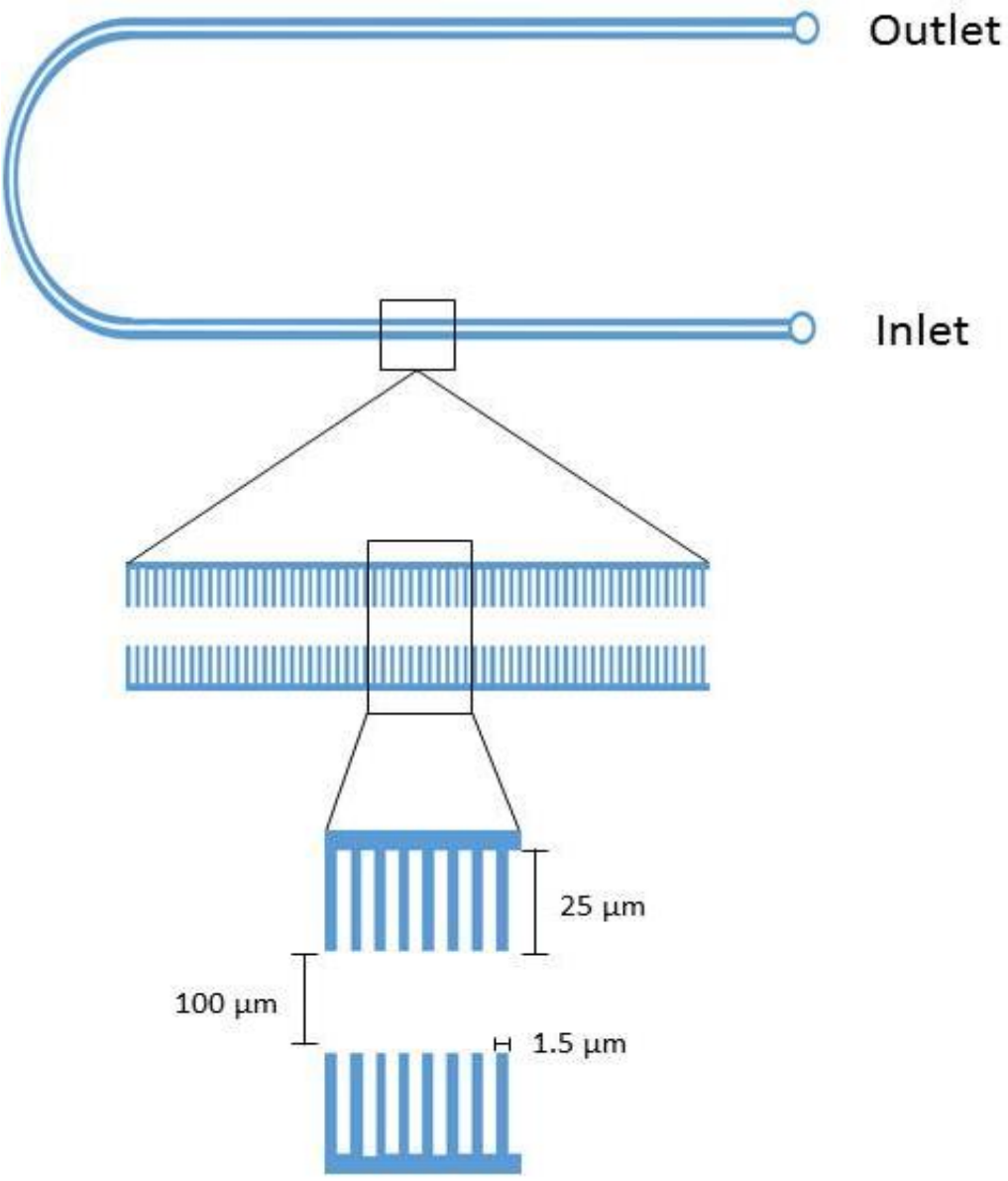

Fig 2.4: The Mother machine chip design. U-shaped main channel (25 µm of depth, 100 µm of width) of which one side is equipped with 8000 lateral channels (1.5 µm of width, 1.5 µm of depth, 25 µm of length).

2.2.3 PDMS chip production

The designs above were transferred on photoresist-silicon masters by Dr Pagliara multilevel photolithography.

2.2.3.1 Microfluidic device fabrication

PDMS prepolymer (Sylgard® 184, Dow Corning, Midland, MI) and curing agent were carefully mixed in a 9:1 ratio and let it rest 30 minutes. The solution was cast over the master, let it rest for additional 30 minutes to remove all air bubbles and placed in an oven at 70 °C for 120 minutes. The cured PDMS replica was separated from the master by cutting and peeling it off, and inlets and outlets were created using a biopsy puncher with an inner diameter of 0.75mm (World Precise Instrument, Irvine, UK). The PDMS replica was irreversibly sealed on a glass coverslip by exposing both surfaces to oxygen plasma treatment (10 s exposure to 30 W plasma power, Plasma etcher, Diener, Royal Oak, MI, USA).

2.2.4 Microfluidic persister assay

2.2.4.1 Microscope setup

Bright-field and fluorescence images were taken via an Inverted microscope (IX73 Olympus, Tokyo, Japan) at 30 minutes intervals to measure cells growth. The microscope was equipped with a 60× magnification, 1.2 N.A. objective (UPLSAPO60XW, Olympus, Tokyo, Japan) and a sCMOS camera (Zyla 4.2, Andor, Belfast, UK). The device was moved by two automated stages (M-545.USC and P-545.3C7, Physik Instrumente, Karlsruhe, Germany, for coarse and fine movements, respectively). For fluorescence imaging, a Broad-spectrum LED (CoolLED pE300white, Andover, UK) and filter cubes were used.

2.2.4.2 Bacteria staining

For monitoring the viability of single bacteria and the membrane integrity of the cell rapid epifluorescence staining method using the LIVE/DEAD Bacterial Viability Kit (Thermo Fisher Scientific, Gloucester, UK) was applied to as described in the protocol supplied by the manufactures. Briefly, BacLight is composed of two nucleic acid-binding stains: SYTO 9 and propidium iodide (PI). SYTO 9 penetrates all bacterial membranes and stains the cells green, while PI only penetrates cells with damaged membranes, and the combination of the two stains produces red fluorescing cells. Optimal incubation conditions were found to be 30 minutes, at room temperature in the dark. Total (red + green) and viable (green) cells can hence be counted (Boulos et al., 1999).

2.2.4.3 Microfluidic-based persister assay

An overnight culture of *E. coli* was cultured for 17 hours in LB (see section 2.1.3). The mother machine (MM) chip was prepared according to section 2.2.3.1. The oxygen plasma treatment temporarily rendered PDMS and glass hydrophilic, so within 5 minutes after bonding the chip was filled with 10 µL of Bovine Serum Albumin, BSA, (50 mg/mL). The BSA passively adsorbs on the PDMS surface avoid the interaction of biomolecules and microfluidic substrates (Mark et al., 2010). The MM chip was then incubated at 37 °C for one hour thus passivating the device internal surface and preventing successive cell adhesion. The overnight culture was concentrated by centrifugation for 5 minutes at 4000 rpm, 20°C. The cell pellet was re-suspended to a theoretical concentration of 50 OD_{600} equivalents in 1 mL of spent LB. 1:100 of BSA (50 mg/mL) was added to the re-suspended culture. 10 µL of bacteria/BSA mixture was injected into the MM chip and incubated in the 37 °C incubator for 20 minutes. This incubation step is necessary to facilitate the entrapment of bacteria cells inside the mother machine chip arms. The mother machine chip was connected to a Flow Unit S (Fluigent, Paris, France), as in Fig. 2.5, continuously measuring the flow rate through the device. The applied pressure was controlled by a computerised pressure-based flow control system (MFCS-4C, Fluigent, Paris, France) through the MAESFLO software (Fluigent, Paris, France).

Spent LB was flowed through the main channel until it cleared the excess of bacteria (~5 minutes at 50-250 mbar gradually over this time) shown in Fig. 2.6.

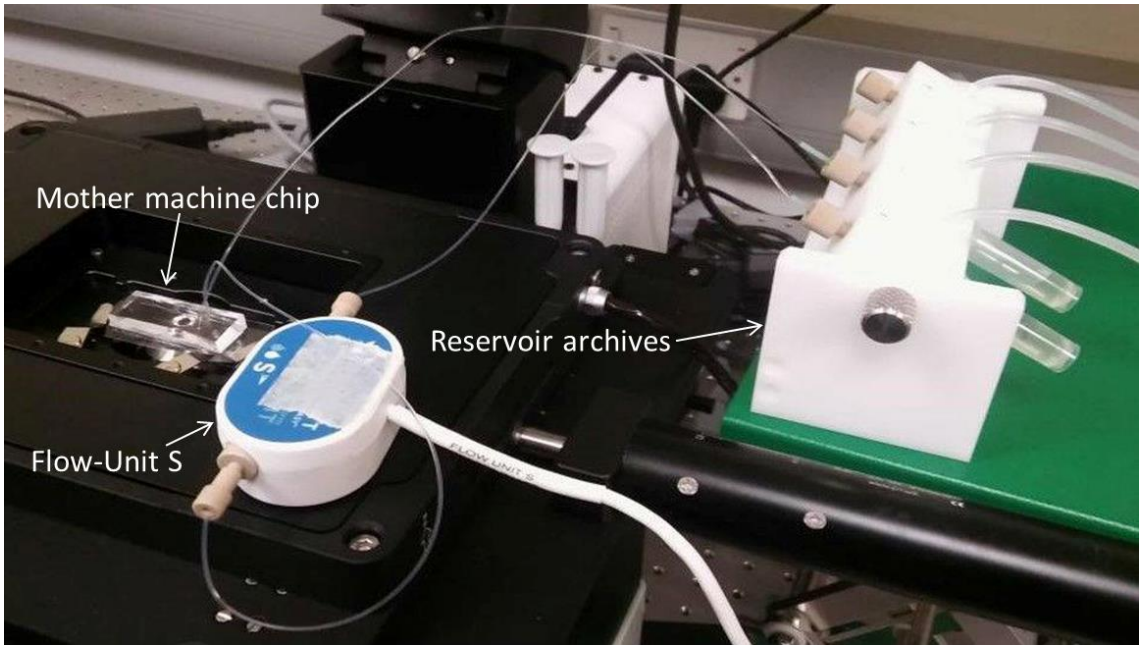

Fig. 2.5: Microfluidics setup mounted on the automated microscope stage. The Mother machine inlet is connected to Flow Unit S feeding from reservoir archives.

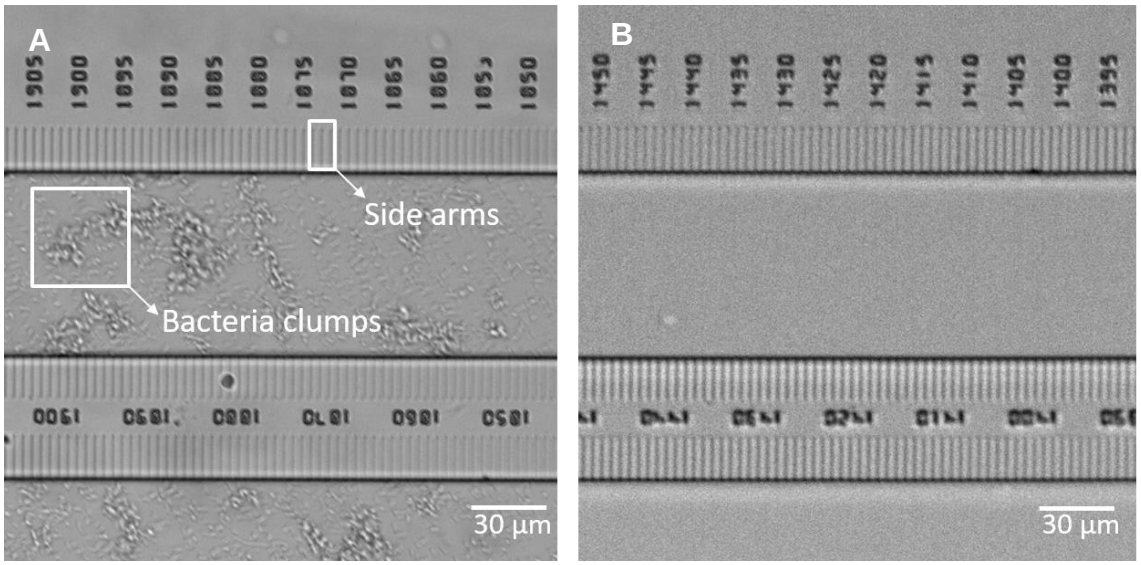

Fig. 2.6: Before and after washing step. Images had taken before (A) and after (B) 5 minutes of washing at 50-250 mbar through the main channel.

Once cleaned the main channel the set up was ready for the experiment. Fresh LB/drugs (25×MIC) was injected through the main channel for three hours and images have been taken every 30 minutes (flow rate 100 µL/hr). After the 3 hours challenge, only fresh LB was given to the bacteria cells to let them re-grow for other 3 hours. Finally, PI/fresh LB and subsequently SYTO9/fresh LB were added. Bright-field and fluorescence images were acquired after 30 minutes of incubation respectively.

2.2.5 Image analysis

The bright field and fluorescence images acquired during and after the antibiotics challenge described in the previous section were analysed using the ImageJ software (Schneider et al. 2012). The background fluorescence of the whole field of view in each fluorescent channel was subtracted from the fluorescence of each cell, at each time point. The average fluorescence intensity of the pixels contained within the specified cell boundaries was determined for each cell and fluorescence channel. Once analysed the whole time's sequence of images was examined visually for cell counting. The cells were sorted based on staining and morphology in dividing, growing, and non-growing (viable but not culturable cells) cell fractions.

2.3 DNA PAINT

2.3.1 Buffers

Table 2.3: A list of the buffers used and their components, pH was adjusted to 7.5.

Buffer	**Composition (for 1 L)**
TE Buffer 1x	10 mM Tris-HCl pH 8 1 mM EDTA
TE Buffer+1 M NaCl	10 mM Tris-HCl pH 8 1 mM EDTA 1 M NaCl
Buffer C	100 mM Sodium Phosphate Buffer 500 mM NaCl 1 mM EDTA

2.3.2 Oligonucleotides Design

All oligonucleotides were purchased from Integrated DNA Technologies (IDT) or Eurofins Genomics as a salt-free pellet. Oligonucleotides were re-suspended in a Tris-EDTA (TE) buffer solution to make a 100 µM solution and stored at -20°C. The docking strands are biotinylated, while imaging is performed using imager strands labelled with the following dyes ATTO655 or ATTO550.

Table 2.4: Oligonucleotides design

	Permanently Binding																								
Docking	Bt	A	G	A	T	G	T	G	A	G	T	G	A	A	G	G	A	G	T	G	T	T	A	G	A	
Complementary Strand		T	C	T	A	C	A	C	T	C	A	C	T	T	C	C	T	C	A	C	A	A	T	C	T	
Imagers								C	T	C	A	C	T	T	C	C	T	C	A	C	A	A	T	C	A	A655/550

*Bt: Biotin; A655/550: Atto655 or Atto550

2.3.3 DNA coating of streptavidin-functionalized colloidal particles

Streptavidin-coated Polystyrene particles have been used, (from microparticles GmbH, Berlin, Germany), with an average diameter of 0.527 µm (10 mg/mL in aqueous solution), stored at 4˚C. For coating colloidal particles with DNA TE buffer + 10 mM NaCl, TE buffer + 100 mM NaCl, TE buffer + 1 M NaCl have been used. Alternatively, phosphate buffer can be used instead of TE buffer.

2.3.4 Optimized coating process

5 µL of colloidal particles solution have been sonicated at room temperature for 10 minutes to break up aggregates. 100 µL of DNA docking strand @1µM (Table 2.3.) have been defrosted and mixed into the 5 µL batch colloidal solution. DNA aliquots contain 100 pmoles of DNA, 4x excess compared to the binding capacity of the particles. DNA-batch colloidal solution has then been vortexed and incubated for 2 hours at RT on a shaker (to prevent sedimentation). Subsequently, the particles have been washed to remove unbound DNA by adding 400 µL of TE buffer with 10 mM NaCl. This reduces the salt concentration to avoid particle aggregation over the next steps. Samples have been centrifuged for 5 minutes at 13.6 k rpm. The supernatant has been removed but the 5 µL at the bottom, which should contain most of the particles. Particles have been re-suspended the in 100 µL of 10 mM NaCl TE buffer and mixed by vortex and then repeated 4 times to get rid of the entire unbound DNA. The particles have been used within 1 or 2 days and Stored in the fridge at 4˚C.

The NaCl concentration was increased gradually to 300 mM by adding small aliquots of 1 M NaCl TE buffer every 30 minutes after the beginning of the incubation. Higher salt concentration improves the binding of the DNA by screening coulomb repulsion but also favours particle aggregation via van der Waals.

2.3.5 Microfluidics chip design

The microfluidic platform was designed as described in section 2.2.2. For this experiment, the DNA-PAINT chip A and B were designed (fig 2.7 A and B).

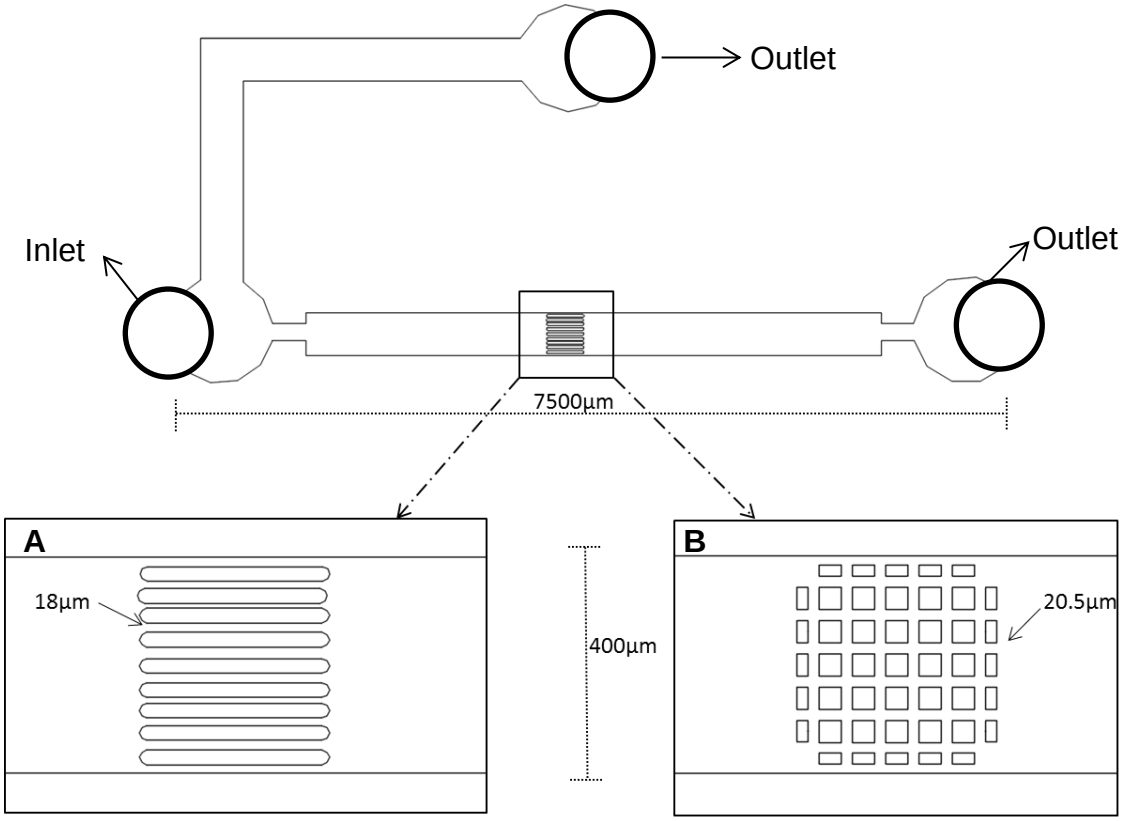

Fig.2.7: The DNA-PAINT chip design of the photomask (top) and its channels (bottom).

2.3.6 Optimisation of microfluidics protocol for DNA paint

Preliminary experiments and optimisation have been executed on a coverslip. Subsequently, a microfluidic chip was designed and moulded (Fig. 2.6). The DNA-PAINT chip A was prepared according to section 2.2.2. The colloidal particles, beads for brevity, coated with DNA (see table 2.4) were injected and let them settle for 30 minutes. DNA-PAINT chip A was connected to two shut off valve (Fig.2.8). The inlet reservoir was filled with Buffer C, which was flowed (50 mbar) through the main channel to wash away the excess of beads. In order to change solution, the pressure was reduced to zero, and the imager A655 (1nM) (see table 2.4) was injected. Images were acquired, and then the sample was

washed through the microfluidic chip with Buffer C. Finally, the second imager, A550, was added, and images were acquired.

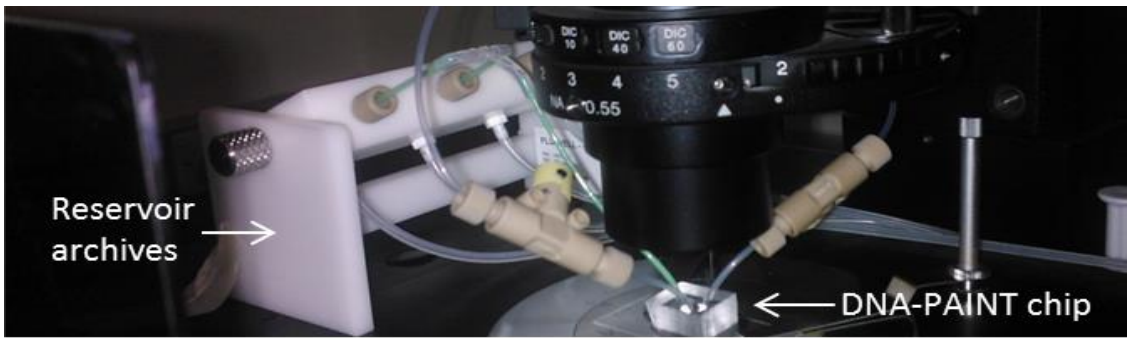

Fig.2.8: Microfluidics setup for DNA-PAINT. DNA-PAINT chip attached to the shut-off valve, connected to the reservoir archives and microfluidics pump.

3. Results

3.1 Classic Microbiological assays

In this section the results from classic microbiology assays have be presented. Here the temporal windows in cell growth cycles, during which, in response to antibiotics a culture became enriched for persisters cells have been identified. Three antibiotics were tested: a β-lactam (ampicillin), an aminoglycoside (gentamycin) and a fluoroquinolone (ofloxacin). At first, E. coli cells were treated for three hours at 25× their MIC for ampicillin, gentamicin or ofloxacin, diluted in fresh LB medium and the corresponding fraction of persisters cell identified. Then, the same experiment has been performed, with the antibiotics supplemented with a medium spent by the growing bacterial culture itself in order to evaluate how the persisters fraction behaves in this stress-inducing environment.

3.1.1 Growth stage dependent persister cells formation

The *E. coli* culture showed a growth phase-dependent division rate (Fig. 3.1). After 30 minutes from dilution of an overnight culture in LB, the cell division rate was close to zero and then slowly increased to a maximal value of 2.8±0.4 div h^{-1} after 3.5 hours from dilution. After this time, the division rate decreased to a value close to zero.

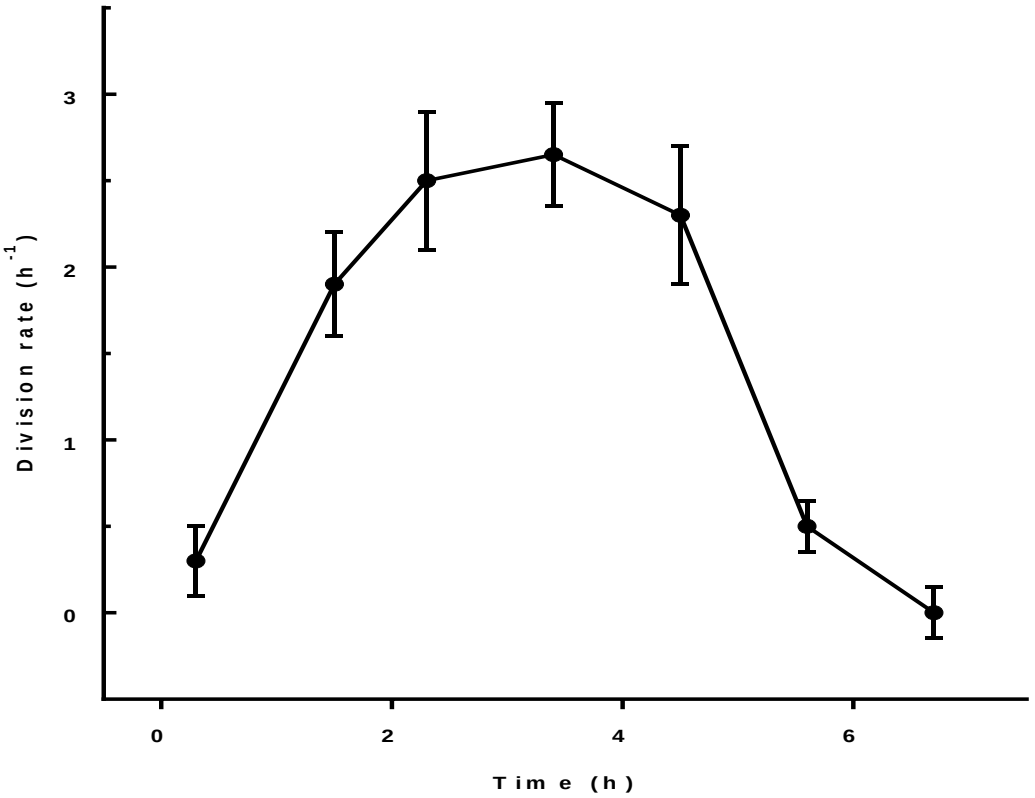

Fig. 3.1: The bacterial division rate throughout the different stages of growth. An overnight culture of *E. coli* BW25113 was diluted 1:1000 in fresh LB. We measure division rate as the log 2 fold change between the bacterial colony forming unit CFU at consecutive hourly intervals throughout a bacterial growth cycle. Measurements and SEM are calculated from at least three biological and technical replicates.

3.1.2. Effect of the environment on persister cell formation

In order to study the growth-state dependence of persistence, we used the protocol described in section 2.1.4.2. For this experiment, a culture of *E. coli* was treated for three hours at given time points with ampicillin, gentamicin or ofloxacin. We found that the absolute number of persister cells increased during growth and became constant as the culture entered stationary phase (Fig.3.2).

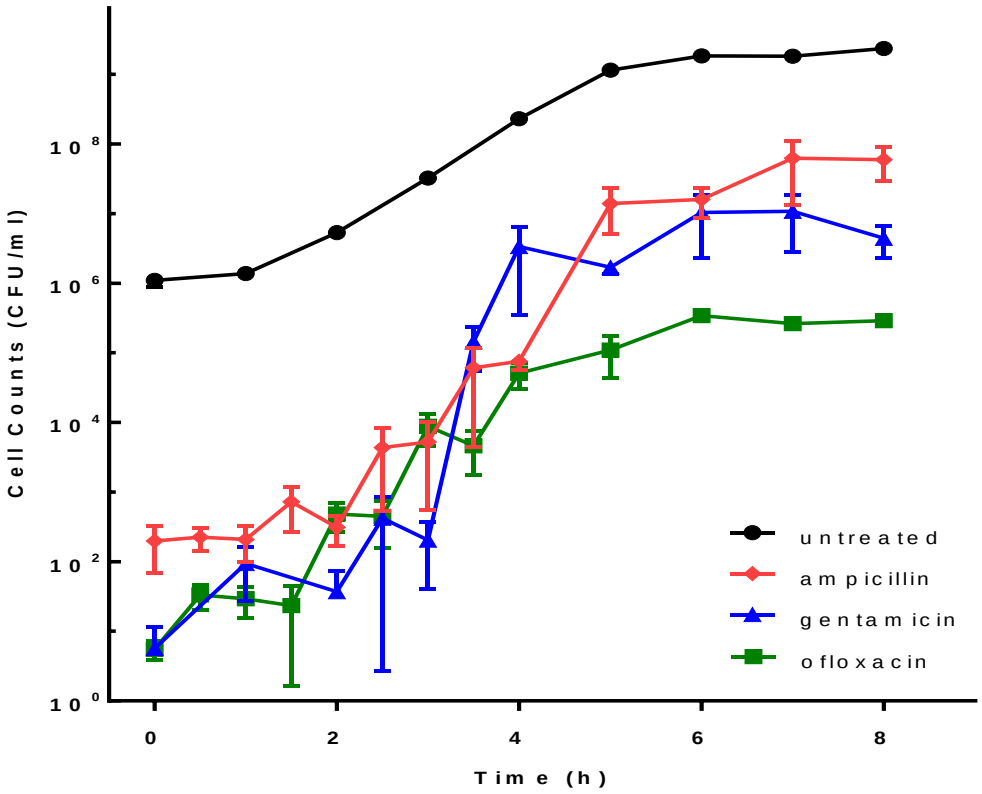

Fig. 3.2: Number of persister cells in a population tracked after three hours treatment with three different antibiotics. Dependence of the number of persister cells to ampicillin (red diamond), gentamicin (blue triangle), or ofloxacin (green square) on time elapsed from dilution in LB medium. Corresponding counts for the total number of bacteria in the culture before antibiotic treatment (black circles). Data and error bars are the mean and standard error of the mean (SEM) of measurements obtained by using the colony forming unit (CFU) assay at least on biological triplicates as described in section 2.1.4.2. Drugs were administered for three hours at 25x MIC.

For each drug and each time point, we performed two different treatments as illustrated in Fig. 2.1 c: three culture aliquots were treated with the drug and fresh LB (Fig. 2.1c, ii) whereas three other aliquots were treated with drug only

solubilised in ddH_2O (Fig. 2.1c, iii). In both cases, the final drug concentration was 25× the drug MIC.

When ampicillin only was added to the culture aliquots, we measured a 1.5 $\log_{10}$ fold increase in the fraction of persister cells one hour after dilution from overnight culture (t=1 h, Fig 3.3 open symbols). At the same time point we did not observe any increase of persister cells when we added ampicillin in fresh LB to the aliquots; however, in the same case, we measured a 2 log10 fold increase during the interval 4-7 hours (full symbols in Fig. 3.3).

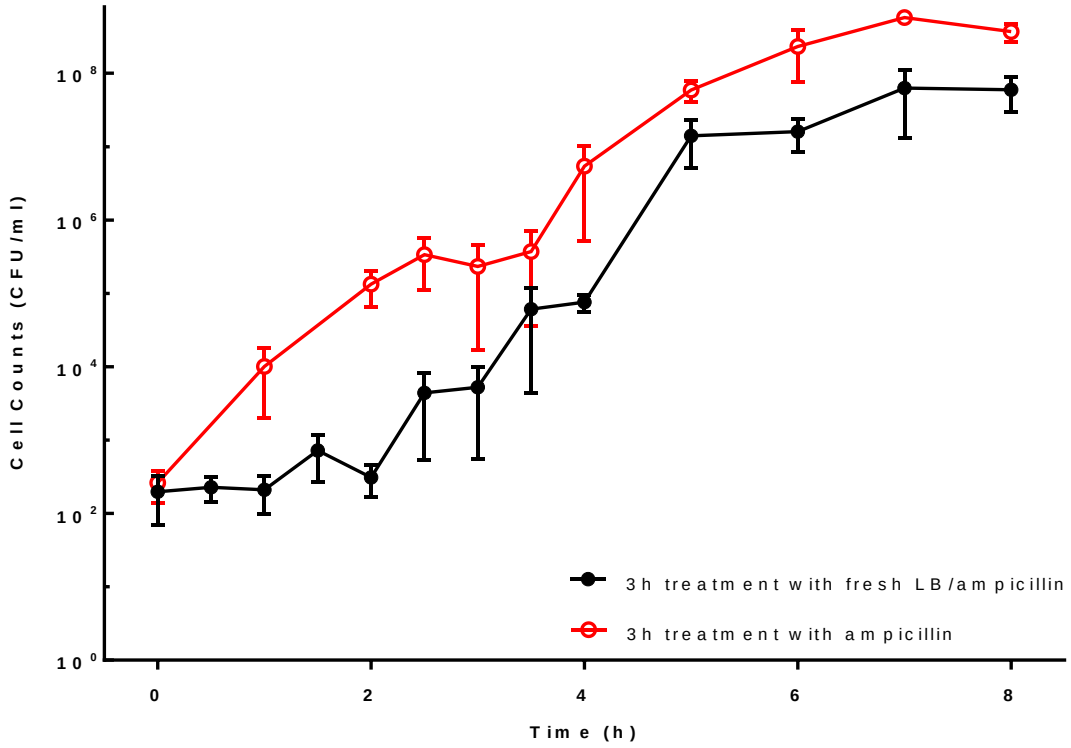

Fig 3.3: Three hours treatment with ampicillin. Dependence of the number of persister cells to ampicillin on time elapsed from dilution in LB medium. Data and error bars are the mean and standard error of the mean (SEM) of measurements obtained by using the colony forming unit (CFU) assay at least on biological triplicates as described in section 2.1.4.2. Drugs were administered for three hours at 25×MIC.

When gentamicin only was added to the culture aliquots, the persister cells growth curve showed a 3.6 $\log_{10}$ fold increase between t=2 hours and t=3 hours, before remaining relatively constant for the remainder of the growth cycle (Fig 3.4 open symbols). The fraction of persisters to gentamicin when the antibiotic was added with fresh LB showed a similar pattern, except for a shift of 1 hour, with a 3.4 log10 fold increase between t=3 hours and t=4 hours.

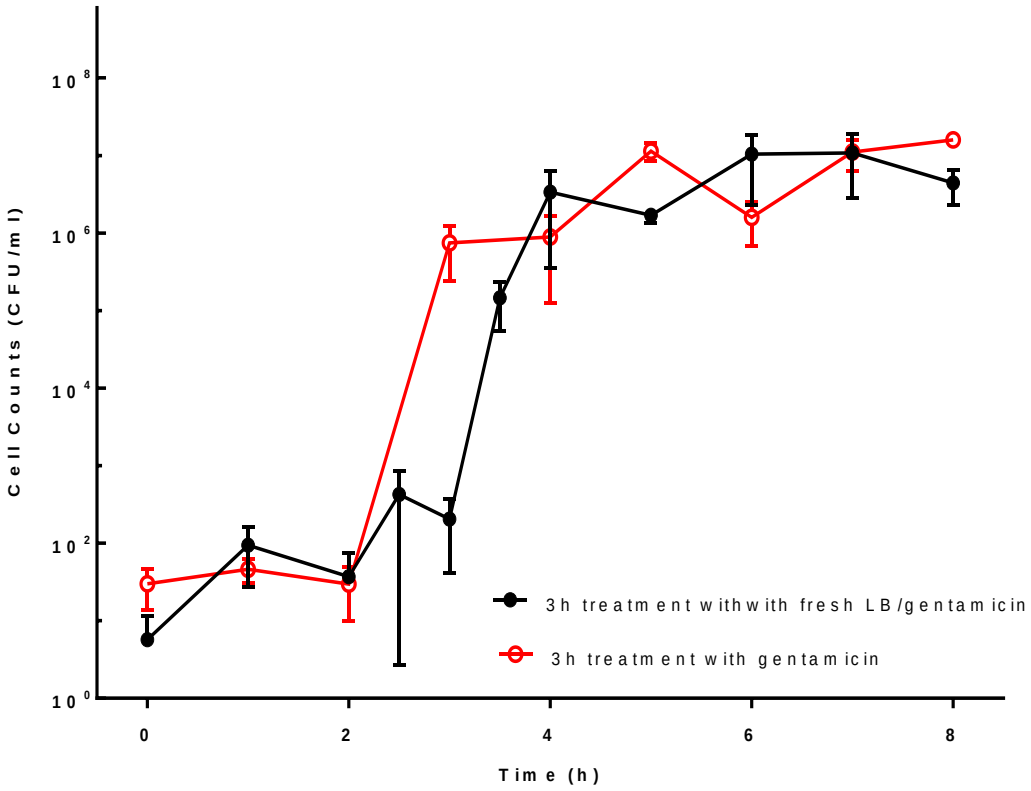

Fig. 3.4: Three hours treatment with gentamicin. Dependence of the number of persister cells to ampicillin on time elapsed from dilution in LB medium. Data and error bars are the mean and standard error of the mean (SEM) of measurements obtained by using the colony forming unit (CFU) assay at least on biological triplicates as described in section 2.1.4.2. Drugs were administered for three hours at 25×MIC.

When ofloxacin was added to the aliquots with fresh LB there was little change in the persister cells throughout the growth cycle (Fig. 3.5 closed symbols). However, the persister fraction showed a 2.6 $\log_{10}$ fold increase between t=2 hours and t=4 hours was found when ofloxacin only was added to the culture aliquots (Fig. 3.5 open symbols).

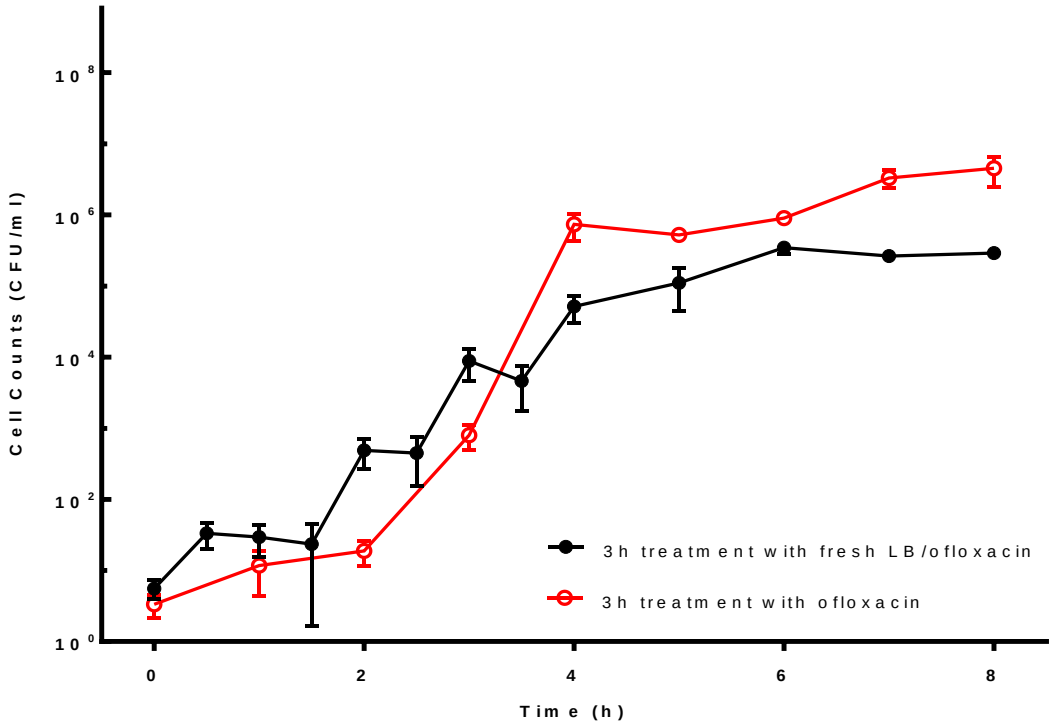

Fig 3.5: Three hours treatment with ofloxacin. Dependence of the number of persister cells to ampicillin on time elapsed from dilution in LB medium. Data and error bars are the mean and standard error of the mean (SEM) of measurements obtained by using the colony forming unit (CFU) assay at least on biological triplicates as described in section 2.1.4.2. Drugs were administered for three hours at 25×MIC.

The differences in the persister cells fraction between the two treatment methods suggest that persister formation is strongly affected by the environment.

3.1.3 Role of *ompF* on persister cell formation

To evaluate the role of *ompF* in the formation of persister cells an *E. coli* knock-out mutant Δ*ompF* was used to repeat the three hours challenge assay. The *ompF* gene encodes one of the major outer membrane porins that have been associated with drug uptake (Cama et al., 2015; Delcour, 2009; Ziervogel, 2013).

A comparison between the persister cells curve in the WT and Δ*ompF* (Fig 3.6), did not show significant differences.

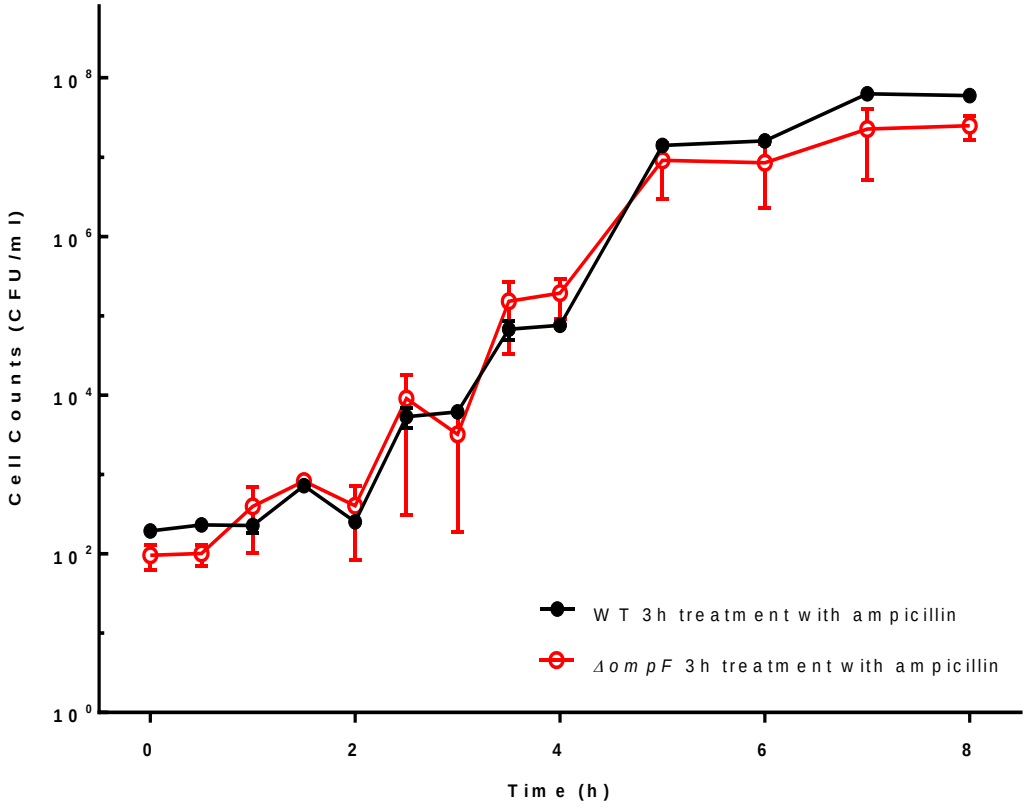

Fig. 3.6: Dependence of the number of persister cells to ampicillin on time elapsed from dilution in LB medium. Data and error bars are the mean and standard error of the mean (SEM) of measurements obtained by using the colony forming unit (CFU) assay at least on biological triplicates as described in section 2.1.4.2. Drugs were administered for three hours at 25×MIC.

When the Δ*ompF* was treated for three hours with gentamicin showed a similar pattern compared to the WT except for a steep increase shifted of 1 hour, no more between 3 and 4 hours but between 4 and 5 hours (Fig. 3.7).

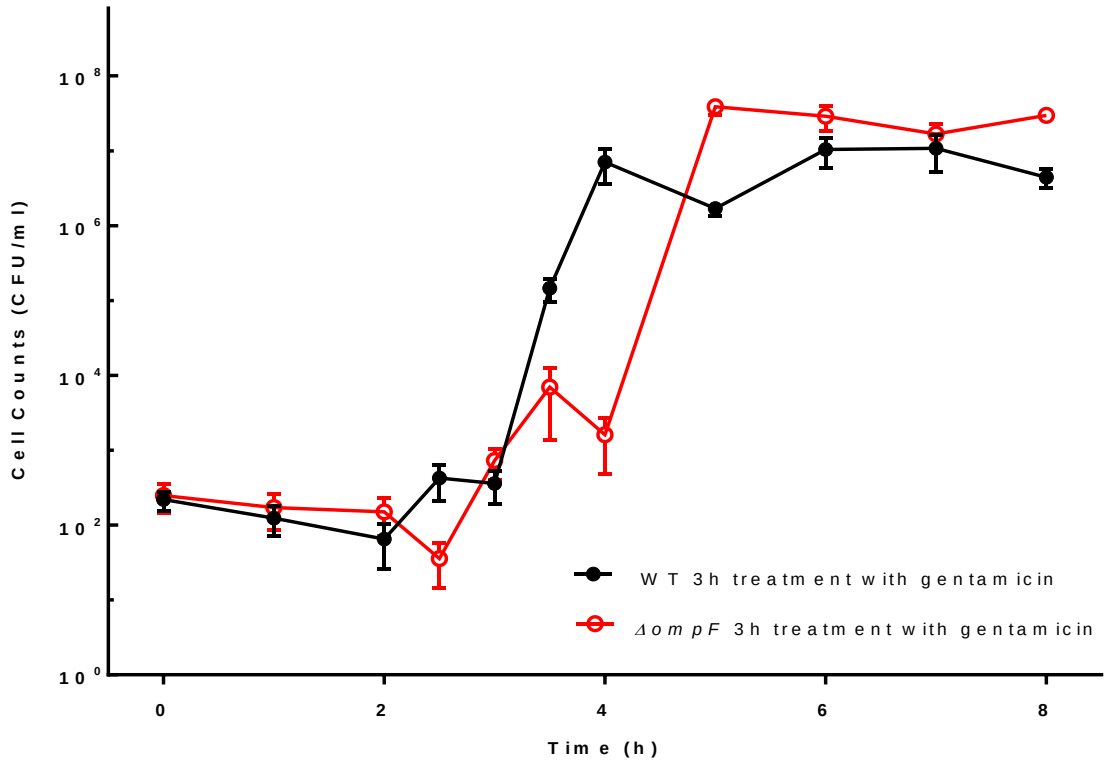

Fig. 3.7: Dependence of the number of persister cells to ampicillin on time elapsed from dilution in LB medium. Data and error bars are the mean and standard error of the mean (SEM) of measurements obtained by using the colony forming unit (CFU) assay at least on biological triplicates as described in section 2.1.4.2. Drugs were administered for three hours at 25×MIC.

When the *ΔompF* was treated for three hours with ofloxacin, we recorded a decrease of persister fraction compared to the WT except for between 7 and 8 hours (Fig. 3.8).

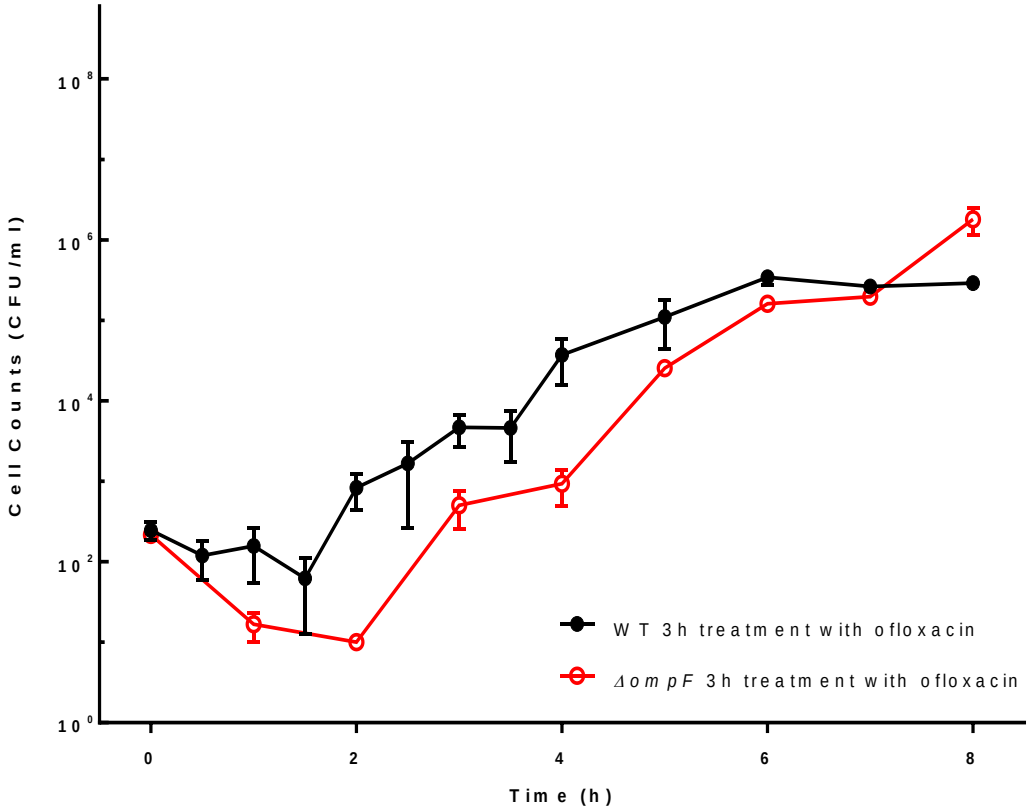

Fig. 3.8: Three hours treatment with ofloxacin. Dependence of the number of persister cells to ampicillin on time elapsed from dilution in LB medium. Data and error bars are the mean and standard error of the mean (SEM) of measurements obtained by using the colony forming unit (CFU) assay at least on biological triplicates as described in section 2.1.4.2. Drugs were administered for three hours at 25×MIC.

3.1.4 Discussion

The dominant model of persistence postulates that persister cells are dormant phenotypic variants of normal cells that form stochastically in microbial populations (Balaban et al., 2004; Lewis, 2010; Maisonneuve et al., 2013). Persister cells can also arise in response to a number of environmental conditions, including nutrient limitation (Maisonneuve & Gerdes, 2014) and nutrient transitions (Amato et al., 2013). During bacterial growth, such environmental conditions are constantly changing, and in addition to this, a population can generate its own native stress, such as nutrient exhaustion or environmental acidification. However, increasing evidence now suggests that only specific environments favour persister cell formation (Amato et al., 2013; Bernier et al., 2013; Keren et al., 2004; Vega et al., 2012).

Results presented here identify the temporal windows in cell growth cycles during which, in response to antibiotics a culture became enriched for persister cells (Fig. 3.2). Three antibiotics of different classes of antibiotic were tested: a β-lactam (ampicillin), a fluoroquinolone (ofloxacin) and an aminoglycoside (gentamycin). At first, *E. coli* cells were treated for three hours at 25× their MIC for ampicillin, gentamicin or ofloxacin, diluted in fresh LB medium and the corresponding fraction of persister cells identified. Following this, the same experiment was performed, with the antibiotics supplemented with a medium spent by the growing bacterial culture itself, in order to evaluate how the persister fraction behaves in this stress-inducing environment. From the results shown in Fig. 3.3 and 3.5, what emerges is that cells treated with antibiotics, but without fresh media regrow at higher density than the cells in the nutrient rich environment. This trend is more evident in treatment with ampicillin and ofloxacin. The comparison between our two treatments helped to understand the importance of the medium composition to the response of sub-populations of bacteria to the antibiotic treatments. Indeed, drug treatment with fresh LB might alter the native culture environment, making cells more active and more susceptible to the drugs. Finally, the role of *ompF* was studied using an *E. coli* knock out *ΔompF*. The *ompF* gene encodes for one of the major outer membrane porins associated with drug uptake (Cama et al., 2015; Delcour, 2009; Ziervogel, 2013). It could be hypothesised that the absence of *ompF* may lead to a reduced drug uptake and increased survival to drug treatment. However, our data do not

show substantial differences between *ΔompF* and WT populations under the investigated conditions (Fig. 3.6, 3.7 and 3.8).

3.2 Microfluidics

3.2.1 Microfluidic-based persister assay

In order to study the persister cell formation by using a microfluidic chip, cells from a stationary phase culture were introduced into the Mother Machine device. The first phase of the experiment (Fig. 3.9 t=0), cells moved from the main channel to the side arms. As soon as the cells settled in the arms (usually within 20 minutes), spent media (section 2.1.1.1) was injected by applying an external pressure (50 to 250 mbar) to remove the excess cells. It is worth to point that with the present technology we are not completely able to control the number of cells trapped in our microfluidic. The number of cells trapped in each experiment has been specified in Table 3.1. In the next step, cells were treated with a 25× MIC concentration of antibiotics (ampicillin, gentamicin or ofloxacin) for 3 hours to isolate persister cells (Fig 3.9 t=0, t=180 minutes). Image analysis revealed that a few cells began to elongate after 90 minutes (Fig. 3.9 t=90 minutes), while others started to lyse after 180 minutes of treatment with ampicillin. During treatment with ofloxacin cells started to elongate after 60 minutes (Fig. 3.11 t=60 minutes), while after 3 hours of gentamicin cells neither grew nor elongated (Fig. 3.10 t=180 minutes). To evaluate the cell's response to a challenge of three hours of incubation with the different antibiotics, the cells were observed for further three hours after the removal of the antibiotics (ampicillin, gentamicin or ofloxacin), during which fresh LB medium was injected continuously (Fig 3.9 t=360 minutes). After 150 minutes, those cells that already had begun to elongate finally divided to produce a micro-colony (Fig 3.9 t=360 minutes). Cells treated with ofloxacin also elongated during washing with LB medium (Fig. 3.11 t=360 minutes), while cells treated with gentamicin neither grew nor elongated (Fig. 3.10 t=360 minutes). The last step was to distinguish live cells from dead cells by live/dead staining (Fig. 3.9 t=420 minutes). Image analysis revealed that after treatment in the presence of ampicillin, 89% of the cells lysed, 6.7% divided, 2.1% elongated, and 2.2% showed no growth. During gentamicin treatment only 59.6% lysed and 40.4% neither divided nor elongated. During the treatment with ofloxacin, 55.7% of cells were registered as susceptible, 0.4% as dividing, 20.7% as elongating, and 23.2% as non-growing cells. This is shown in Table 3.2, with a comparison between bulk and microfluidics studies.

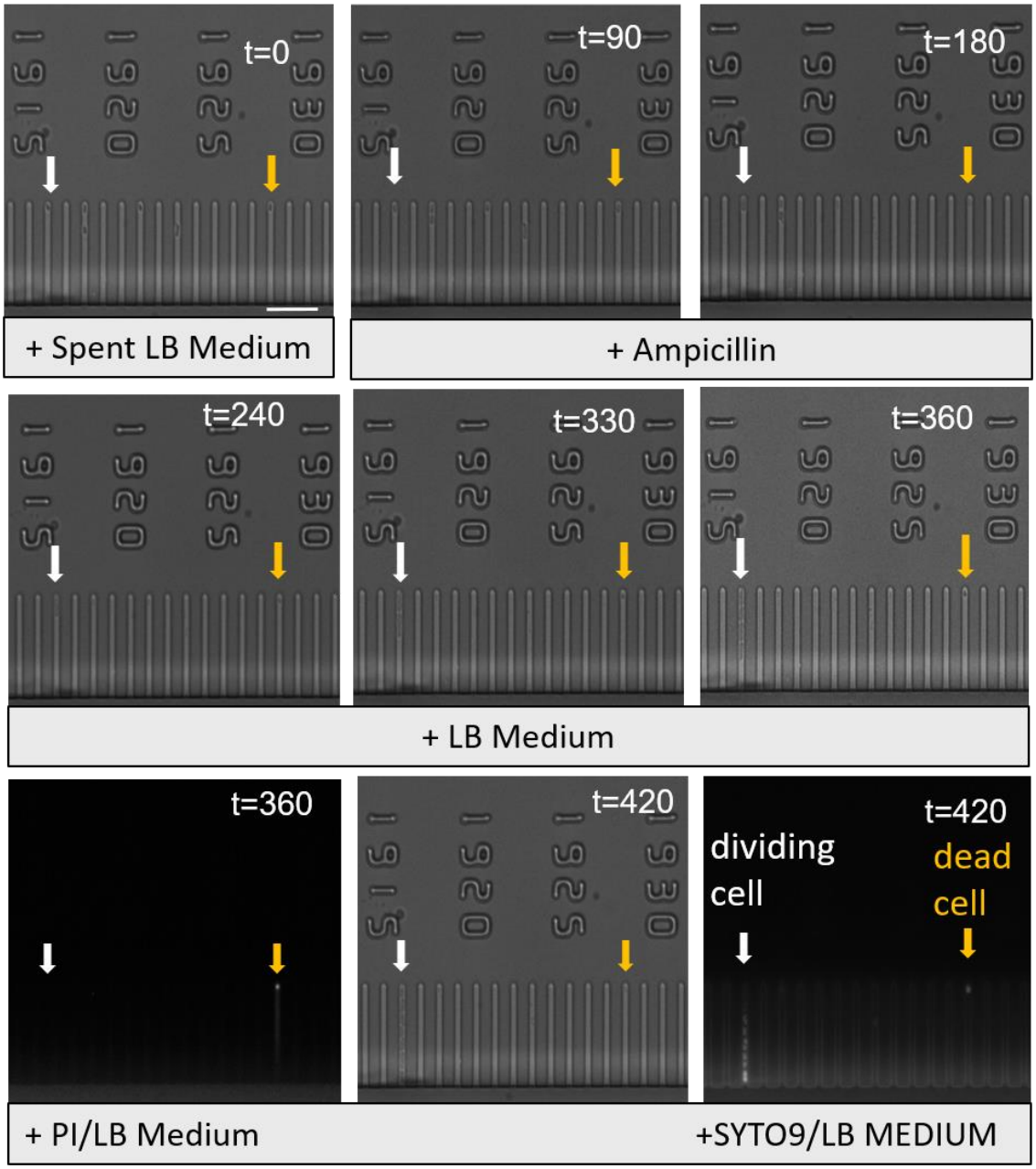

Fig. 3.9: Exponentially growing cells of *E. coli* BW25113 analysed by microfluidics under the effect of ampicillin (see section 2.2.4.3). Time-lapse microscopy images are showing a single growth-arrested and resuscitation cell (white arrow), lysing cells and not lysed but dead cell (golden arrow) during the ampicillin (LB/ampicillin 25× MIC) treatment. (scale bar, 10 µm) (t = time in minutes).

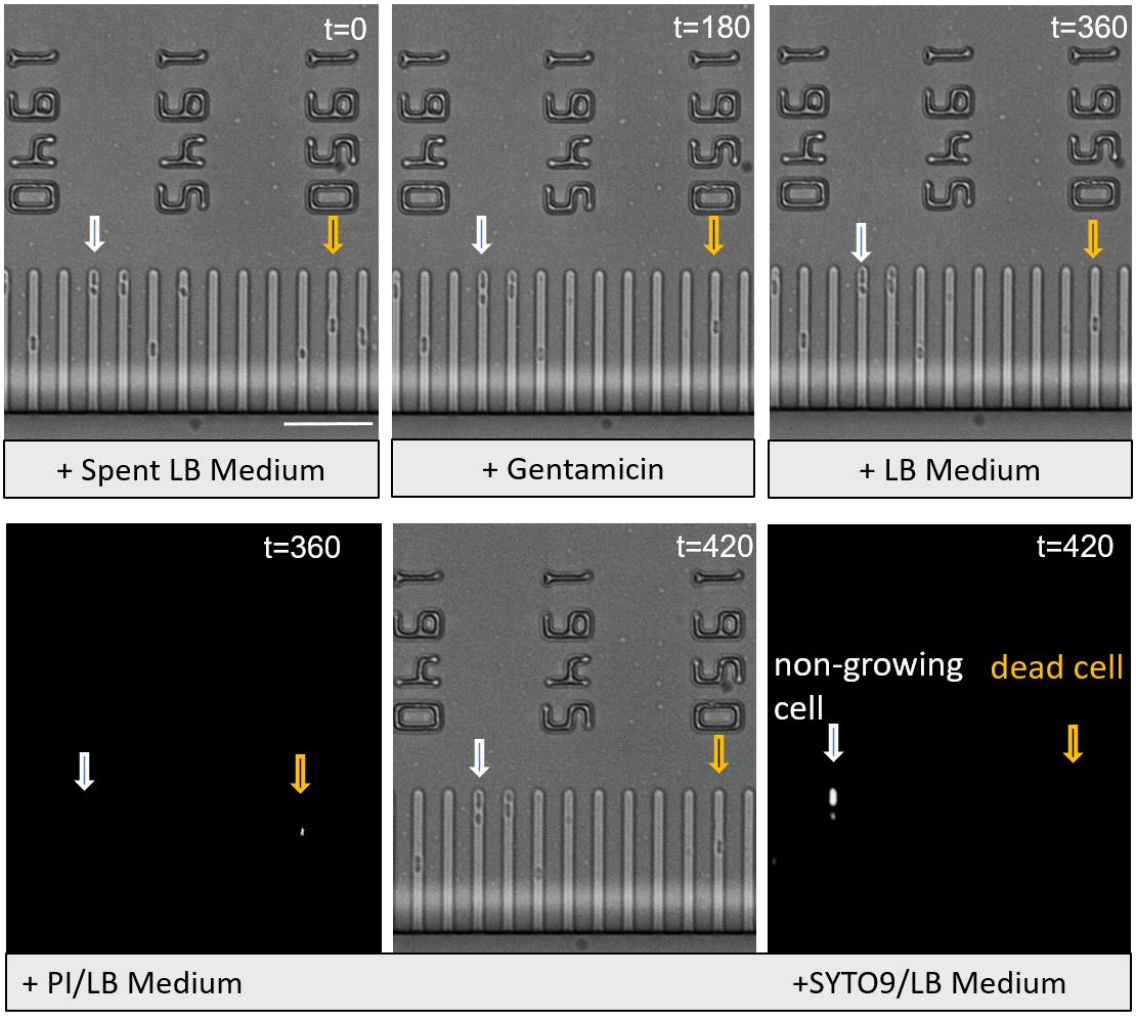

Fig. 3.10: Exponentially growing cells of *E. coli* BW25113 analysed by microfluidics under the effect of gentamicin (see section 2.2.4.3). Time-lapse microscopy images are showing a single growth-arrested cell but alive (white arrow), growth-arrested cell dead (gold arrow) after the gentamicin (LB/gentamicin; 25× MIC) treatment. (scale bar, 10 µm) (t = time in minutes).

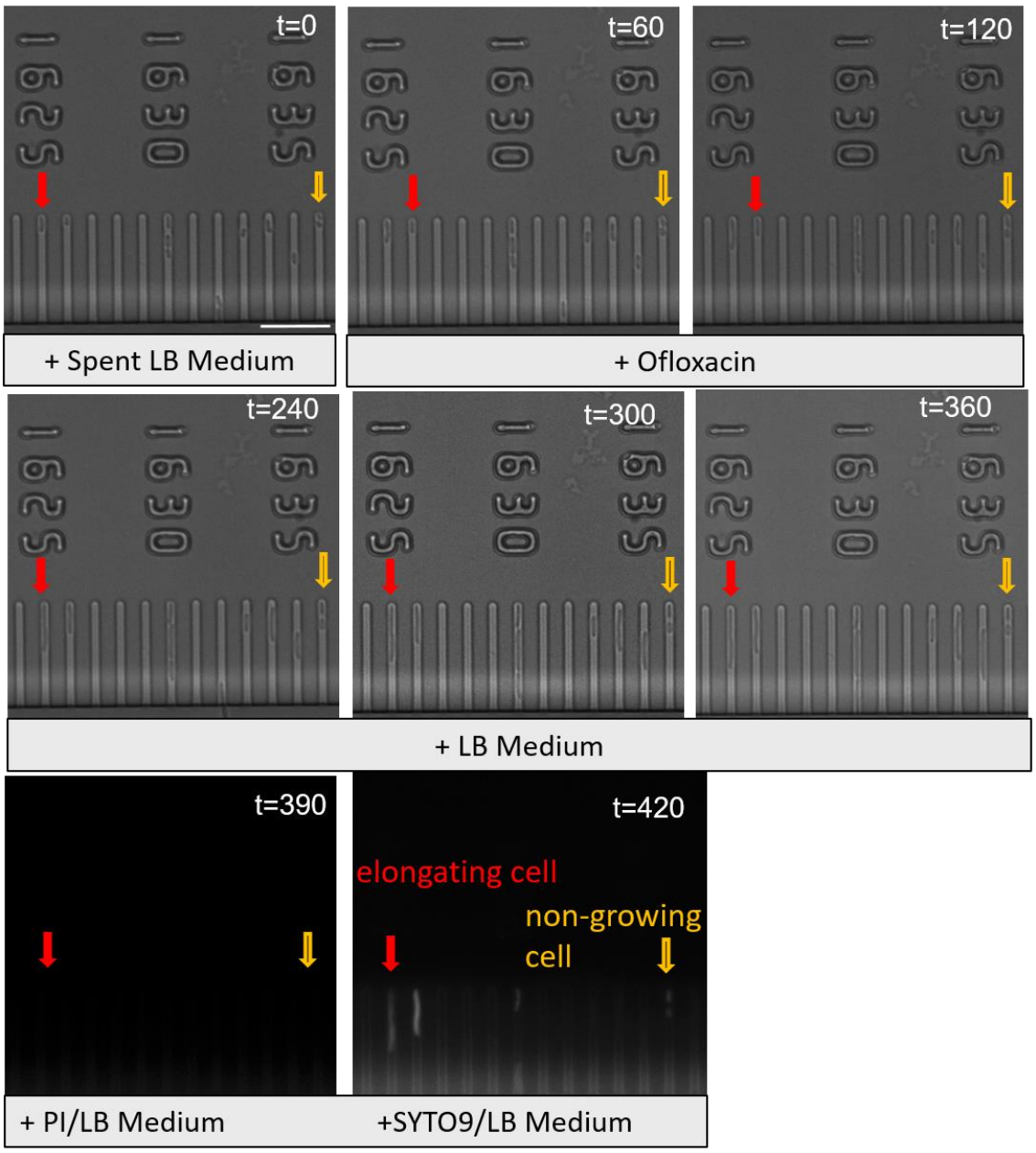

Fig 3.11: Exponentially growing cells of *E. coli* BW25113 analysed by microfluidics under the effect of ofloxacin (see section 2.2.4.3). Time-lapse microscopy images are showing a single elongating cell (red arrow); not lysed but dead cell (golden arrow) during the ofloxacin (LB/ofloxacin; 25× MIC) treatment. (scale bar, 10 µm) (t = time in minutes).

Table 3.1: Comparison between bulk studies and Microfluidics studies

	Planktonic growth (Cell fraction)	Microfluidic growth (Cell fraction)					
Drug	Average dividing cells*	Average dividing cells**	Average susceptible cells**	Average elongating cells**	Average non-growing cells **	Average number of cells/ experiment	Average cell number/channel
Ampicillin	0.187 ± 0.012	0.067 ± 0.014	0.89 ± 0.012	0.021 ± 0.004	0.022 ± 0.01	710	0.497 ± 0.082
Gentamicin	0.007 ± 0.072	0	0.596 ± 0.033	0	0.404 ± 0.041	1807	1.230 ± 0.041
Ofloxacin	0.001 ± 0.047	0.004 ± 0.002	0.557 ± 0.152	0.207 ± 0.066	0.232 ± 0.103	1015	0.689 ± 0.122
Control	N/A	0.950 ± 0.359	0	0.014 ± 0.006	0.034 ± 0.013	722	0.448 ± 0.169

*CFU from a 17 hours culture on LB agar plate; **Microfluidics studies

3.2.2 Discussion

The work presented here shows a new way to study persister cells by using bespoke microfluidics, especially by exploiting the Mother Machine chip to trap cells and allow phenotypic analysis at the single-cell level. Indeed, with standard microbiological techniques we can only measure the persister fraction as shown in Table 3.1, while the combination of microfluidics and microscopy permits us to be able to distinguish additional phenotypes, such as elongating cells (Fig.3.11) or non-growing cells (also called VBNC cells) (Fig. 3.10). This last phenotype is very difficult to isolate. VBNC cells are non-dividing and, unlike persister cells, are unable to immediately regain the ability to divide when plated on routine laboratory medium (Ramamurthy et al., 2014). VBNC cells were thought to be formed after longer periods of incubation in environmental conditions that do not sustain growth. However, a recent study (Ayrapetyan et al., 2015) revealed that VBNC cells can exist together with persister cells in unstressed growing cultures.

Here, three classes of antibiotics have been used to investigate cellular response after three hours of treatment. Although the average number of cells trapped is different for each experiment a trend was observed. Unsurprisingly by comparing the average dividing cells of the control to the average dividing cells treated with the antibiocts the latter resulted to be at least 10 times less numerous than the control (Table 3.1).

Looking at the other data available in Table 3.1 it was possible to note some effects of the different antibiotics on the cells metabolism. In particular, it was observed that a higher percentage (6.4%) of dividing cells occurred during treatment with ampicillin. Ampicillin acts as an irreversible inhibitor of the enzyme transpeptidase, and inhibits the final stage of bacterial cell wall synthesis, ultimately leading to cell lysis. Therefore, it was easy to detect lysed bacteria trapped in the Mother Machine arms. Antibiotics like gentamicin act as protein synthesis inhibitors, thus a microfluidics experiment registered a higher percentage of non-growing bacteria (40%), while ofloxacin acts as an enzyme inhibitor on DNA replication, causing bacteria to elongate or enter a non-growing state (20% and 23% of the population, respectively). This continues until the cells translate all the mRNA available into the cytosol, rendering the cell is unable to grow and replicate, resulting in cell death. Is it possible to observe a small portion

of elongating and non-growing cells also in the control, this is possibly explained by the bet-hedging reported in section 1.1.3.

One of the current limitations in our understanding of persister cells, is that with classic microbiological techniques analysis can only be carried out after treatment with antibiotics, not before, due to a lack of biomarkers to isolate persister cells from the total percentage of susceptible cells in a population before the antibiotic challenge. Moreover with the classic microbiology techniques it is impossible to identify the different cells behaviour. Indeed in Table 3.1 the number of cells in planktonic growth includes all the alive cells that can be distinguished into non-growing and elongating by the application of our microfluidic technique.

It is worth remembering that persister cells are phenotypic variants produced stochastically in a population of cells, and also that their relative abundance can rise, reaching 1%, at the mid to late-exponential phase of growth (2.5 to 5 hours for *E. coli*) (Keren et al., 2004). We also know that they are able to spontaneously switch between persistent and susceptible state regaining sensitivity to antibiotics. Upon switching back, they appear indistinguishable from normal cells (Kussell et al., 2005). Thus cultures grown from persister cells are as sensitive to drugs as the parental culture from which the persisters were derived (Lewis, 2010; Moyed & Bertrand, 1983; Peng et al., 2016). Recent studies (Balaban et al., 2013; Maisonneuve & Gerdes, 2014; Harms et al., 2016) suggest that the reversible adoption of a slowly-growing or non-growing state is regarded as a general strategy of persistence.

3.3 Preliminary results from DNA-PAINT

In this section, the possible application of DNA-PAINT combined with microfluidics has been explored. In this case an example of Exchange PAINT will be described. As mentioned in the introduction, DNA-PAINT is a method that exploits programmable transient hybridisation between short single-stranded oligonucleotide strands, allowing multiplexed, single-molecule and single-label visualisation down to a resolution of ~ 5-10 nm.

For this work, small beads (5 µm) were coated with the desired docking strands (Table 2.4) following the process described in section 2.3.4 and two different imagers were used to show the “Exchange” into a microfluidic chip.

As mentioned before, docking strands are short, single-stranded DNA oligomers, usually 8–10 nucleotides long. In contrast, the imager strand is conjugated to an organic dye and diffuses freely in the imaging buffer. Thanks to their complementary sequence, imager strands can transiently bind to docking strands. During the bound state, imager strands are fixed for an extended amount of time, allowing the camera to accumulate enough photons from the dye to be detected (Schnitzbauer et al., 2017). The beads coated with DNA were injected and allowed to settle in the main channel for 30 minutes (Fig 3.12 A). The inlet reservoir was filled with Buffer C (table 2.3), and flowed through the main channel to wash away excess beads at 50 µL/hr (Fig 3.12 B). Thus, only well attached beads remained into the microfluidics chip and a solution containing the first imager (A650, Table 2.4) was flowed. A bright field and a fluorescent image were acquired (Fig. 3.12 C and D). Then the sample was washed through the microfluidic chip with Buffer C to wash away A650. To demonstrate that Exchange-PAINT is possible with our microfluidic chip, a second imager, A550 (Table 2.4) was added, and images were acquired in bright field and in fluorescence (Fig 3.12 E and F). As expected the beads remained in their position and the second imager was able to interact with the docking strand taking the place of the first imager, showing that is possible an “Exchange” between the two imagers. Indeed, this it’s clearly observable in Fig 3.12 D and Fig 312 F which show the same fluorescent pattern, suggesting a successful exchange between the two imagers.

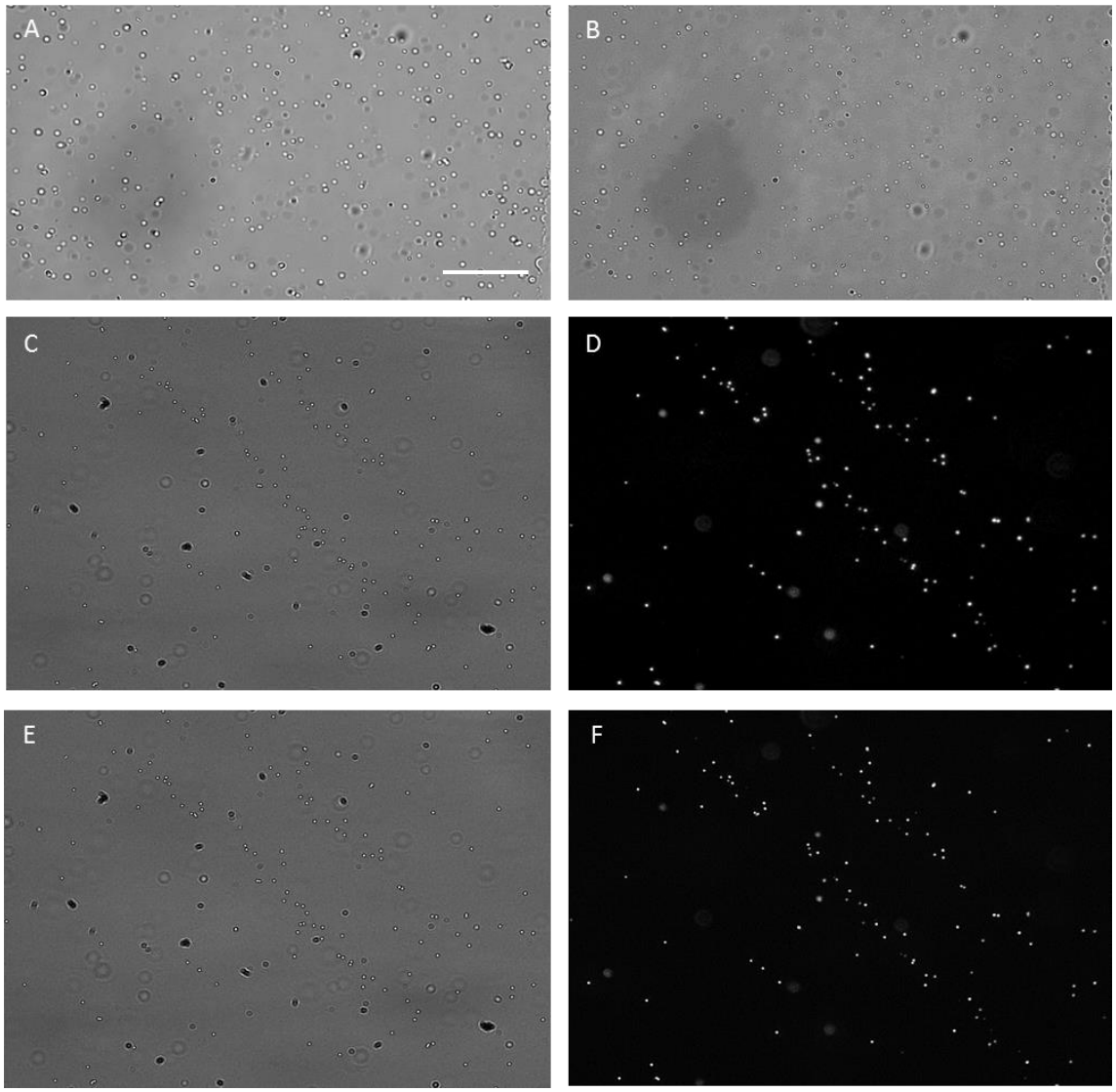

Fig. 3.12: Exchange-PAINT. The beads labelled with docking strands are injected into the microfluidic and let them settle for 30 minutes (A). Buffer C was flowed (50 µL/hr) through the main channel to wash away the excess of beads (B). Brightfield after the addition of the imager A650 (C). The fluorescence was acquired (D). After the acquisition, A650 strands are washed out and exchanged with imager strands A550 (E and F) brightfield and fluorescence respectively. Scale bar: 10µm.

These preliminary results demonstrate the possibility of combining microfluidics and DNA PAINT, to allow control over the sample environment during imaging. By linking docking strands to antibodies, DNA-PAINT can be applied to many *in vitro* and cellular applications. Furthermore, its simplicity enables both novices and expert users to obtain high-quality results quickly. The next step would be to move combine this technique with *in situ* super-resolution microscopy.

4. Summary and future work

Specific environments favour persister cells formation (Amato et al., 2013; Bernier et al., 2013; Keren et al., 2004; Vega et al., 2012). In this work, the temporal windows, in the growth cycle, in which the culture becomes enriched for persister cells to a β-lactam, a fluoroquinolone and an aminoglycoside (Fig. 3.2) were identified. The importance of the medium composition was investigated by comparing two treatments, in the presence and absence of fresh LB medium. The drug treatment with fresh LB altered the native culture environment. For this reason, the next step will be testing different condition such as nutrient transitions and environmental acidification. Moreover, the importance of the treatment duration will be tested by increasing the incubation time with the antibiotics to 24 hours.

Microfluidics studies showed the importance of continuous imaging of single cells. During this work, a protocol for performing persister cell assays in the chip was optimised. The Mother Machine chip is able to trap bacteria allowing microscopic analysis of the persistence phenotype at the single-cell level. Thanks to the microfluidics a complete control over the environmental conditions was achieved while keeping track of single cells. Future works will include the study of metabolic activity, the replication of the starvation studies with microfluidics and the identification (and isolation) of persister cells without drugs challenge.

The preliminary data on DNA-PAINT combined with microfluidics showed that the Exchange-PAINT is possible also with our microfluidic device. The next step will be to adapt the microfluidics setup to a Super-resolution microscope. This will deepen the study of putative persistence protein targets to better understand the molecular mechanisms underlying persistence. Moreover, several in vitro experiments could be designed: from localisation of a specific gene to the identification of a target protein. Once improved the protocol increasingly detailed molecular studies opening the way to multiple molecular biology and cellular application.

5 Bibliography

Abraham, E. P., & Chain, E. (**1940**). An Enzyme from Bacteria able to Destroy Penicillin. *Nature*, *146*(3713), 837–837.

Agasti, S. S., Wang, Y., Schueder, F., Sukumar, A., Jungmann, R., & Yin, P. (**2017**). DNA-barcoded labeling probes for highly multiplexed Exchange-PAINT imaging. *Chem. Sci.*, *8*(4), 3080–3091.

Alanis, A. J. (**2005**). Resistance to antibiotics: Are we in the post-antibiotic era? *Archives of Medical Research*, *36*(6), 697–705.

Alekshun, M. N., & Levy, S. B. (**2007**). Molecular Mechanisms of Antibacterial Multidrug Resistance.

Amato, S. M., Orman, M. A., & Brynildsen, M. P. (**2013**). Article Metabolic Control of Persister Formation in Escherichia coli. *Molecular Cell*, *50*(4), 475–487.

American Hospital Formulary Service Drug Information (AHFS DI). (**2006**).

Appelbaum, P. C. (**2006**, January). MRSA - The tip of the iceberg. *Clinical Microbiology and Infection*. Elsevier.

Ayrapetyan, M., Williams, T. C., Baxter, R., & Oliver, J. D. (**2015**). Viable but nonculturable and persister cells coexist stochastically and are induced by human serum. *Infection and Immunity*, *83*(11), 4194–4203.

Ayrapetyan, M., Williams, T. C., & Oliver, J. D. (**2016**, January). Bridging the gap between viable but non-culturable and antibiotic persistent bacteria. *Trends in Microbiology*.

Balaban, N. Q., Gerdes, K., Lewis, K., & McKinney, J. D. (**2013**). A problem of persistence: still more questions than answers? *Nature Reviews. Microbiology*, *11*(8), 587–91.

Balaban, N. Q., Merrin, J., Chait, R., Kowalik, L., & Leibler, S. (**2004**). Bacterial Persistence a Phenotypic Switch. *Science*, *305*(September), 1622–1625.

Bernier, S. P., Lebeaux, D., Defrancesco, A. S., Valomon, A., Ghigo, J., & Beloin, C. (**2013**). Starvation , Together with the SOS Response , Mediates High Biofilm-Specific Tolerance to the Fluoroquinolone Ofloxacin, *9*(1).

Bhattacharya, S., Datta, A., Berg, J. M., & Gangopadhyay, S. (**2005**). Studies on surface wettability of poly(dimethyl) siloxane (PDMS) and glass under oxygen-plasma treatment and correlation with bond strength. *Journal of Microelectromechanical Systems*, *14*(3), 590–597.

Bigger, J. (**1944**). Treatment Of Staphylococcal Infections With Penicillin By Intermittent Sterilisation. *The Lancet*, *244*(6320), 497–500.

Blondeau, J. M. (**1999**). Expanded activity and utility of the new fluoroquinolones: A review. *Clinical Therapeutics*, *21*(1), 3–40.

Boothe, D. (**2012**). *The Merck Veterinary Manual*.

Boulos, L., Prevost, M., Barbeau, B., Coallier, J., & Desjardi, R. (**1999**). LIVE /

DEAD BacLightE : application of a new rapid staining method for direct enumeration of viable and total bacteria in drinking water. *Journal of Microbiological Methods*, *37*, 77–86.

Brauner, A., Fridman, O., Gefen, O., & Balaban, N. Q. (**2016**). Distinguishing between resistance, tolerance and persistence to antibiotic treatment. *Nature Reviews Microbiology*, *14*(5), 320–330.

Brock David C. (**2011**). A measure of success.

Cama, J., Bajaj, H., Pagliara, S., Maier, T., Braun, Y., Winterhalter, M., & Keyser, U. F. (**2015**). Quanti fi cation of Fluoroquinolone Uptake through the Outer Membrane Channel OmpF of Escherichia coli.

Campos, M., Surovtsev, I. V., Kato, S., Paintdakhi, A., Beltran, B., Ebmeier, S. E., & Jacobs-Wagner, C. (**2014**). A constant size extension drives bacterial cell size homeostasis. *Cell*, *159*(6), 1433–1446.

Choi, K., Ng, A. H. C., Fobel, R., & Wheeler, A. R. (**2012**). Digital microfluidics. *Annual Review of Analytical Chemistry (Palo Alto, Calif.)*, *5*, 413–40.

Chukwudi, C. U. (**2016**). rRNA binding sites and the molecular mechanism of action of the tetracyclines. *Antimicrobial Agents and Chemotherapy*.

Chung, H. S., Yao, Z., Goehring, N. W., Kishony, R., Beckwith, J., & Kahne, D. (**2009**). Rapid beta-lactam-induced lysis requires successful assembly of the cell division machinery. *Proceedings of the National Academy of Sciences of the United States of America*, *106*(51), 21872–21877.

Churchman, L. S., Okten, Z., Rock, R. S., Dawson, J. F., & Spudich, J. A. (**2005**). Single molecule high-resolution colocalization of Cy3 and Cy5 attached to macromolecules measures intramolecular distances through time. *Proceedings of the National Academy of Sciences of the United States of America*, *102*(5), 1419–23.

Cruickshank, M., Duguid, M., Gotterson, F., & Carter, D. (**2014**). Taking action to preserve the miracle of antibiotics. *Australian Veterinary Journal*, *92*(1–2), 3–7.

Delcour, A. H. (**2009**). Biochimica et Biophysica Acta Outer membrane permeability and antibiotic resistance. *BBA - Proteins and Proteomics*, *1794*(5), 808–816.

Dubnau, D., & Losick, R. (**2006**). Bistability in bacteria. *Molecular Microbiology*, *61*(3), 564–572.

Duffy, D. C., McDonald, J. C., Schueller, O. J. A., & Whitesides, G. M. (**1998**). Rapid prototyping of microfluidic systems in poly(dimethylsiloxane). *Analytical Chemistry*, *70*(23), 4974–4984.

Eliopoulos, G. M., Willey, S., Reiszner, E., Spitzer, P. G., Caputo, G., & Moellering, R. C. (**1986**). In vitro and in vivo activity of LY 146032, a new cyclic lipopeptide antibiotic. *Antimicrobial Agents and Chemotherapy*, *30*(4), 532–535.

Eurofins Scientific. (**2017**). Retrieved July 31, 2017, from http://www.eurofins.com/biopharma-services/discovery/?_ga=2.137310004.586467563.1501498594-2042740561.1501498594

Finberg, R., Fingeroth, J., in Longo, D., Fauci, A., Kasper, D., Hauser, S., & Jameson, J. (**2012**). *Harrison's Principles of Internal Medicine* (18th ed.). McGraw-Hill.

Firmino, N., Goldsmith, J., & Morin, A. (**2013**). Ampicillin Resistance Is Increased in Escherichia coli K12 relA and spoT Mutants but Sub-inhibitory Pretreatment Does Not Induce Adaptive Resistance, *17*(April), 34–39.

Fischer, J., & Robin Ganellin, C. (**2006**). Analogue-based Drug Discovery. *Analogue-Based Drug Discovery*, (December), 1–575.

Flors, C., Ravarani, C. N. J., & Dryden, D. T. F. (**2009**). Super-resolution imaging of DNA labelled with intercalating dyes. *ChemPhysChem*, *10*(13), 2201–2204.

Fridman, O., Goldberg, A., Ronin, I., Shoresh, N., & Balaban, N. Q. (**2014**). Optimization of lag time underlies antibiotic tolerance in evolved bacterial populations. *Nature*, *513*(7518), 418–421.

Gordon, M. P., Ha, T., & Selvin, P. R. (**2004**). Single-molecule high-resolution imaging with photobleaching. *Proceedings of the National Academy of Sciences of the United States of America*, *101*(17), 6462–6465.

Guo, M. T., Rotem, A., Heyman, J. A., & Weitz, D. A. (**2012**). Droplet microfluidics for high-throughput biological assays. *Lab on a Chip*, *12*(12), 2146.

Guo, X., Murray, M., Xiong, C., & Zhu, S. (**2013**). Treatment of Escherichia coli BW25113 with Subinhibitory Levels of Kanamycin Results in Antibiotic Cross-Resistance and TolC Upregulation, *17*(April), 19–23.

Hansen, S., Lewis, K., & Vulic, M. (**2008**). Role of Global Regulators and Nucleotide Metabolism in Antibiotic Tolerance in Escherichia coli □, *52*(8), 2718–2726.

Harms, A., Maisonneuve, E., & Gerdes, K. (**2016**). Mechanisms of bacterial persistence during stress and antibiotic exposure. *Science*, *354*(6318), aaf4268.

Harrison, D. J., Fluri, K., Seiler, K., Fan, Z., Effenhauser, C. S., & Manz, A. (**1993**). Micromachining a Miniaturized Capillary Electrophoresis-Based Chemical Analysis System on a Chip. *Science*, *261*(5123), 895–897.

Hathorn, E., Dhasmana, D., Duley, L., & Ross, J. D. (**2014**). The effectiveness of gentamicin in the treatment of Neisseria gonorrhoeae: a systematic review, *3*, 1–9.

Holtje, J. V. (**1998**). Growth of the stress-bearing and shape-maintaining murein sacculus of Escherichia coli. *Microbiology and Molecular Biology Reviews : MMBR*, *62*(1), 181–203.

Hooper, D. C. (**1999**). Mechanisms of fluoroquinolone resistance. *Drug Resistance Updates*, *2*(1), 38–55.

Horne, D., & Tomasz, A. (**1977**). Tolerant response of Streptococcus sanguis to beta-lactams and other cell wall inhibitors. *Antimicrobial Agents and Chemotherapy*, *11*(5), 888–896.

Huang, B., Bates, M., & Zhuang, X. (**2009**). Super-resolution fluorescence microscopy. *Annual Review of Biochemistry*, *78*, 993–1016.

Huang, K. C., Mukhopadhyay, R., Wen, B., Gitai, Z., & Wingreen, N. S. (**2008**). Cell shape and cell-wall organization in Gram-negative bacteria. *Proceedings of the National Academy of Sciences of the United States of America*, *105*(49), 19282–7.

Hussain, T. (**2015**). Pakistan at the verge of potential epidemics by multi-drug resistant pathogenic bacteria. *Adv. Life Sci. 2*.

Jungmann, R., Avendano, M. S., Woehrstein, J. B., Dai, M., & Shih, W. M. (**2014**). Multiplexed 3D Cellular Super-Resolution Imaging with DNA-PAINT and Exchange-PAINT, *11*(3), 313–318.

Kampranis, S. C., & Maxwell, A. (**1998**). Conformational changes in DNA gyrase revealed by limited proteolysis. *J Biol Chem*, *273*(35), 22606–22614.

Kawahara, S. (**1998**). Chemotherapeutic agents under study. *Nihon rinsho. Japanese journal of clinical medicine*, *56*(12), 3096–3099.

Kedzierska, B., & Hayes, F. (**2016**). Emerging roles of toxin-antitoxin modules in bacterial pathogenesis. *Molecules*, *21*(6).

Keren, I., Kaldalu, N., Spoering, A., Wang, Y., & Lewis, K. (**2004**). Persister cells and tolerance to antimicrobials, *230*, 13–18.

Kester, J. C., & Fortune, S. M. (**2014**). Persisters and beyond: Mechanisms of phenotypic drug resistance and drug tolerance in bacteria. *Critical Reviews in Biochemistry and Molecular Biology*, *49*(2), 91–101.

Kohanski, M. A., Dwyer, D. J., & Collins, J. J. (**2010**). How antibiotics kill bacteria: from targets to networks. *Nature Reviews. Microbiology*, *8*(6), 423–35.

Kussell, E. (**2005**). Bacterial Persistence: A Model of Survival in Changing Environments. *Genetics*, *169*(4), 1807–1814.

Kussell, E., & Leibler, S. (**2005**). Phenotypic Diversity, Population Growth, and Information in Fluctuating Environments. *Science*, *309*(5743), 2075–2078.

Lacoste, T. D., Michalet, X., Pinaud, F., Chemla, D. S., Alivisatos, A. P., & Weiss, S. (**2000**). Ultrahigh-resolution multicolour colocalization of single fluorescent probes. *Proceedings of the National Academy of Sciences of the United States of America*, *97*(17), 9461–6.

Lagerholm, B. C., Averett, L., Weinreb, G. E., Jacobson, K., & Thompson, N. L. (**2006**). Analysis Method for Measuring Submicroscopic Distances with Blinking Quantum Dots. *Biophysical Journal*, *91*(8), 3050–3060.

Lerner, P. I. (**2004**). Producing penicillin. *The New England Journal of Medicine*, *351*(6), 524.

Levin, B. R., & Rozen, D. E. (**2006**). Non-inherited antibiotic resistance. *Nature Reviews Microbiology*, *4*(7), 556–562.

Levison, M. (**2012**). *The Merk Manual*.

Lewis, K. (**2010**). Persister Cells. *Annual Review of Microbiology*, *64*(1), 357–372.

Lewis, K. (**2013**). Platforms for antibiotic discovery. *Nature Reviews Drug Discovery*, *12*(5), 371–87.

Lidke, K., Rieger, B., Jovin, T., & Heintzmann, R. (**2005**). Superresolution by localization of quantum dots using blinking statistics. *Optics Express*, *13*(18), 7052–7062.

Ma, C., Sim, S., Shi, W., Du, L., Xing, D., & Zhang, Y. (**2009**). Escherichia coli.

Madou, M. J. (**2002**). *Fundamentals of microfabrication : the science of miniaturization*. CRC Press.

Mairhofer, J., Roppert, K., & Ertl, P. (**2009**). Microfluidic Systems for Pathogen Sensing: A Review. *Sensors*, *9*(6), 4804–4823.

Maisonneuve, E., Castro-Camargo, M., & Gerdes, K. (**2013**). (p)ppGpp controls bacterial persistence by stochastic induction of toxin-antitoxin activity. *Cell*, *154*(5), 1140–1150.

Maisonneuve, E., & Gerdes, K. (**2014**). Review Molecular Mechanisms Underlying Bacterial Persisters. *Cell*, *157*(3), 539–548.

Marians, K. J., & Hiasa, H. (**1997**). Mechanism of quinolone action. A drug-induced structural perturbation of the DNA precedes strand cleavage by topoisomerase IV. *Journal of Biological Chemistry*, *272*(14), 9401–9409.

Mark, D., Haeberle, S., Roth, G., Von Stettenz Ab, F., & Zengerlez, R. (**2010**). Microfluidic lab-on-a-chip platforms: requirements, characteristics and applications, *954*(14).

Mingeot-Leclercq, M. P., Glupczynski, Y., & Tulkens, P. M. (**1999**). Aminoglycosides: Activity and resistance. *Antimicrobial Agents and Chemotherapy*, *43*(4), 727–737.

Moerner, W. E., & Kador, L. (**1989**). Optical detection and spectroscopy of single molecules in a solid. *Physical Review Letters*, *62*(21), 2535–2538.

Mohan, R., Mukherjee, A., Sevgen, S. E., Sanpitakseree, C., Lee, J., Schroeder, C. M., & Kenis, P. J. A. (**2013**). A multiplexed microfluidic platform for rapid antibiotic susceptibility testing. *Biosensors and Bioelectronics*, *49*, 118–125.

Moyed, H. S., & Bertrand, K. P. (**1983**). hipA, a newly recognized gene of Escherichia coli K-12 that affects frequency of persistence after inhibition of murein synthesis. *Journal of Bacteriology*, *155*(2), 768–75.

Nelson, J. M., Chiller, T. M., Powers, J. H., & Angulo, F. J. (**2007**). Fluoroquinolone-resistant Campylobacter species and the withdrawal of fluoroquinolones from use in poultry: a public health success story. *Clinical Infectious Diseases : An Official Publication of the Infectious Diseases Society of America*, *44*, 977–980.

Orrit, M., & Bernard, J. (**1990**). Single pentacene molecules detected by fluorescence excitation in a p-terphenyl crystal. *Physical Review Letters*, *65*(21), 2716–2719.

Pan, X. S., & Fisher, L. M. (**1997**). Targeting of DNA gyrase in Streptococcus pneumoniae by sparfloxacin: Selective targeting of gyrase or topoisomerase IV by quinolones. *Antimicrobial Agents and Chemotherapy*, *41*(2), 471–474.

Partridge, D. G. (**2009**). The Oxford Handbook of Infectious Diseases and Microbiology. *Journal of Infection*, *59*(5), 376.

Payne, D. J., Gwynn, M. N., Holmes, D. J., & Pompliano, D. L. (**2007**). Drugs for bad bugs: confronting the challenges of antibacterial discovery. *Nat Rev Drug Discov*, *6*(1), 29–40.

Peng, C., Tao, X., Wenhong, Z., & Ying, Z. (**2016**). Molecular mechanisms of bacterial persistence and phenotypic antibiotic resistance. *Yi Chuan = Hereditas*, *38*(10), 859–871.

Pinto, D., Santos, M. A., & Chambel, L. (**2015**). Thirty years of viable but nonculturable state research: Unsolved molecular mechanisms. *Critical Reviews in Microbiology*, *41*(1), 61–76.

Pollack, M. G., Fair, R. B., & Shenderov, A. D. (**2000**). Electrowetting-based actuation of liquid droplets for microfluidic applications. *Applied Physics Letters*, *77*(82), 1725–1726.

Qu, X., Wu, D., Mets, L., & Scherer, N. F. (**2004**). Nanometer-localized multiple single-molecule fluorescence microscopy. *Proceedings of the National Academy of Sciences of the United States of America*, *101*(31), 11298–303.

Ramalho, T., Meyer, A., Mückl, A., Kapsner, K., Gerland, U., & Simmel, F. C. (**2016**). Single Cell Analysis of a Bacterial Sender-Receiver System. *PLOS ONE*, *11*(1), e0145829.

Ramamurthy, T., Ghosh, A., Pazhani, G. P., & Shinoda, S. (**2014**). Current Perspectives on Viable but Non-Culturable (VBNC) Pathogenic Bacteria. *Frontiers in Public Health*, *2*.

Wise, B. Y. E. M., & Park, J. T. (**1965**). Synthesis.1-', *54*, 75–81.

Saleh-Lakha, S., & Trevors, J. T. (**2010**). Perspective: Microfluidic applications in microbiology. *Journal of Microbiological Methods*, *82*(1), 108–111.

Sauer-Budge, A. F., Mirer, P., Chatterjee, A., Klapperich, C. M., Chargin, D., & Sharon, A. (**2009**). Low cost and manufacturable complete microTAS for detecting bacteria. *Lab on a Chip*, *9*(19), 2803.

Schneider, C. A., Rasband, W. S., & Eliceiri, K. W. (**2012**). NIH Image to

ImageJ: 25 years of image analysis. *Nature Methods*, *9*(7), 671–5.

Schnitzbauer, J., Strauss, M. T., Schlichthaerle, T., Schueder, F., & Jungmann, R. (**2017**). Super-resolution microscopy with DNA-PAINT.

Schoen, I., Ries, J., Klotzsch, E., Ewers, H., & Vogel, V. (**2011**). Binding-activated localization microscopy of DNA l. *Nano Letters*, *11*(9), 4008–4011.

Scholar, E. M., & Pratt, W. B. (**2000**). *The Antimicrobials Drugs*. Oxford Univ. Press.

Sia, S. K., & Whitesides, G. M. (**2003**). Microfluidic devices fabricated in Poly(dimethylsiloxane) for biological studies. *Electrophoresis*, *24*(21), 3563–3576.

Smith, A., Pennefather, P. M., Kaye, S. B., & Hart, C. A. (**2001**). Fluoroquinolones. *Drugs*, *61*(6), 747–61.

Spratt, B. G. (**1975**). Distinct penicillin binding proteins involved in the division, elongation, and shape of Escherichia coli K12. *Proceedings of the National Academy of Sciences*, *72*(8), 2999–3003.

Taheri-Araghi, S., Brown, S. D., Sauls, J. T., McIntosh, D. B., & Jun, S. (**2015**). Single-Cell Physiology. *Annual Review of Biophysics*, *44*(1), 123–142.

Tipper, D. J., & Strominger, J. L. (**1965**). Mechanism of action of penicillins: a proposal based on their structural similarity to acyl-D-alanyl-D-alanine. *Proceedings of the National Academy of Sciences of the United States of America*, *54*(4), 1133–1141.

Van Oijen, A. ., Köhler, J., Schmidt, J., Müller, M., & Brakenhoff, G. (**1998**). 3-Dimensional super-resolution by spectrally selective imaging. *Chemical Physics Letters*, *292*(1–2), 183–187.

Vega, N. M., Allison, K. R., Khalil, A. S., & Collins, J. J. (**2012**). HHS Public Access, *8*(5), 431–433.

Vulto, P., Dame, G., Maier, U., Makohliso, S., Podszun, S., Zahn, P., & Urban, G. A. (**2010**). A microfluidic approach for high-efficiency extraction of low molecular weight RNA. *Lab on a Chip*, *10*(5), 610–616.

Walsh, C. (**2003**). Antibiotics: Actions, Origins, Resistance. ASM Press.

Wang, P., Robert, L., Pelletier, J., Dang, W. L., Taddei, F., Wright, A., & Jun, S. (**2010**). Robust growth of escherichia coli. *Current Biology*, *20*(12), 1099–1103.

Wen, Y., Behiels, E., & Devreese, B. (**2017**). Toxin-Antitoxin systems : their role in persistence, biofilm formation, and pathogenicity, (October), 240–249.

Whitesides, G. M., Ostuni, E., Jiang, X., & Ingber, D. E. (**2001**). Soft Lithography in Biology and Biochemistry. *Annual Review of Biomedical Engineering*, *3*, 335–73.

World Health Organization (WHO). (**2013**). Model list of essential medicines, *18*(March).

Xia, Y., & Whitesides, G. M. (**1998**). Soft Lithography. *Annual Review of Materials Science*, *28*(1), 153–184.

Xu, H.-S., Roberts, N., Singleton, F. L., Attwell, R. W., Grimes, D. J., & Colwelp, R. R. (**1982**). Survival and Viability of Nonculturable Escherichia coli and Vibrio cholerae in the Estuarine and Marine Environment. *Microb. Ecol*, *8*, 313–323.

Yager, P., Edwards, T., Fu, E., Helton, K., Nelson, K., Tam, M. R., & Weigl, B. H. (**2006**). Microfluidic diagnostic technologies for global public health. *Nature*, *442*(7101), 412–418.

Yehezkel, B. T., Rival, A., Raz, O., Cohen, R., Marx, Z., Camara, M., … Shapiro, E. (**2016**). Synthesis and cell-free cloning of DNA libraries using programmable microfluidics. *Nucleic Acids Research*, *44*(4), e35.

Yildiz, A. (**2003**). Myosin V Walks Hand-Over-Hand: Single Fluorophore Imaging with 1.5-nm Localization. *Science*, *300*(5628), 2061–2065.

Zechiedrich, E. L., & Cozzarelli, N. R. (**1995**). a, 2859–2869.

Ziervogel, B. K. (**2013**). Article The Binding of Antibiotics in OmpF Porin, 76–87.